Microform-scale variations in peatland permeability and their ecohydrological implications

Andy J. Baird[1]*, Alice M. Milner[2], Antony Blundell[1], Graeme T. Swindles[1], and Paul J. Morris[1]

[1]School of Geography, University of Leeds, Leeds, LS2 9JT, United Kingdom

[2]Department of Geography, Royal Holloway, University of London, Egham, Surrey, TW20 0EX, United Kingdom

*Correspondence author. E-mail: a.j.baird@leeds.ac.uk

Running headline: Fine-scale lateral variation in peatland permeability

Supporting information: Appendices S1-S5

Summary

1. The acrotelm-catotelm model of peatland hydrological and biogeochemical processes posits that the permeability of raised bogs is largely homogenous laterally but varies strongly with depth through the soil profile; uppermost peat layers are highly permeable while deeper layers are, effectively, impermeable.

2. We measured down-core changes in peat permeability, plant macrofossil assemblages, dry bulk density and degree of humification beneath two types of characteristic peatland microform – ridges and hollows – at a raised bog in Wales. Six ^{14}C dates were also collected for one hollow and an adjacent ridge.

3. Contrary to the acrotelm-catotelm model, we found that deeper peat can be as highly permeable as near-surface peat and that its permeability can vary by more than an order of magnitude between microforms over horizontal distances of 1-5 metres.

4. Our palaeo-ecological data paint a complicated picture of microform persistence. Some microforms can remain in the same position on a bog for millennia, growing vertically upwards as the bog grows. However, adjacent areas on the bog (< 10 m distant) show switches between microform type over time, indicating a lack of persistence.

5. *Synthesis.* We suggest that the acrotelm-catotelm model should be used cautiously; spatial variations in peatland permeability do not fit the simple patterns suggested by the model. To understand how peatlands as a whole function both hydrologically and ecologically it is necessary to understand how patterns of peat physical properties and peatland vegetation develop and persist.

Key-words: acrotelm-catotelm model, ecological memory, microform, peatland, permeability, persistence, plant–soil (below-ground) interactions, raised bog.

Introduction

Problem statement and research questions

Raised bogs occur commonly in the tropics and at latitudes greater than 45°, especially in the Northern Hemisphere (Ingram 1983; Winston 1994). They are an important global carbon (C) store, and there is interest in how they function as ecosystems and in how they will be affected by climate change; as the climate warms, will they degrade and release their stored C back to the atmosphere, thereby re-enforcing current warming, or will they show some degree of resilience (Swindles *et al*. 2012)? To answer such questions it is necessary to understand how these peatlands behave as ecological and hydrological entities. Conceptually, raised bogs are often divided into two distinct functional layers: (i) an upper acrotelm (literally 'topmost marsh' – see Ingram (1978)) which is the zone in which most water moves and in which biogeochemical processes are most active; and (ii) a lower, poorly-permeable, and usually thicker catotelm in which water flow is slow or negligible and where biogeochemical processes occur at much lower rates (Ingram 1978). While raised bogs undoubtedly show strong vertical variations in peat properties and process rates (e.g. Morris, Baird & Belyea 2015), the usefulness of the simple acrotelm-catotelm dichotomy has been questioned. Morris *et al*. (2011), for example, noted that the model makes the inflexible assumption that a range of biogeochemical and hydrological processes vary in the same binary way with depth. In addition, despite some empirical support for the model, there are quite substantial gaps in our understanding of its applicability. In this paper, we address three questions relating to the model:

(i) is so-called 'catotelm' peat poorly-permeable as assumed by the model?,

(ii) does the permeability of this deeper peat vary laterally between microforms?, and

(iii) how are spatial patterns in permeability related to microform persistence and explained by ecological memory?

Below, we provide a rationale for our focus on these questions.

Background and rationale

Ingram (1978) credited Ivanov (1953) with being the first to propose the concepts of acrotelm and catotelm, although Ivanov (1953, 1981) himself suggested the binary model was established by others before him. Despite emphasising the importance of vertical variations in peat properties, Ivanov (1981) also recognised that peatlands can exhibit distinct lateral variability. Horizontal patterning of peatland microforms (sometimes known as microhabitats or Scale Level 1 features – see Baird, Belyea & Morris (2009)) is seen on many raised bogs. For example, in mid- and high-latitude raised bogs, arrays of hummocks, lawns, and hollows (*sensu* Belyea & Clymo 2001) are common. Hummocks may be *c*. 0.05-0.6 m higher than adjacent hollows and lawns. They are typically 1-3 m in diameter, while the intervening lawns and hollows are often larger, although there is considerable variation in size. These microforms have characteristic plant assemblages. Hummocks tend to be dominated by ericaceous shrubs such as *Calluna vulgaris* (see Appendix S1 in Supporting Information for botanical authorities and common English names) and *Rhododendron groenlandicum*, sedges such as *Eriophorum vaginatum*, and small-leaved Sphagna such as *Sphagnum fuscum* and *Sphagnum capillifolium*. Lawns and hollows have a cover of larger-leaved Sphagna such as *Sphagnum papillosum*, *Sphagnum pulchrum*, and *Sphagnum cuspidatum*, with sedges such as *Rhynchospora alba* often co-dominant. (The species listed here may be found in peatlands in northwest Europe and parts of northeast USA and southeast Canada, and are examples only.) Because peat is the decomposing remains of plants, variations in the composition of the vegetation growing on a bog can be expected to produce variations in peat type; as a bog grows, different types of peat will build up under different types of vegetation.

Lateral variations in the peat under different vegetation types have been described using both direct observation and non-invasive geophysical methods. For example, in a palaeo-ecological study of a raised bog in northern England, Barber (1981) showed how hummocks and intervening lawns and hollows may persist over millenia as a peatland grows. He also suggested that lawns and hollows expand laterally during wet climatic phases and shrink during drier phases (when

hummocks expand), a suggestion made previously by Aaby (1976). Barber (1981) studied peat faces produced by peat cutters from which lateral variations in peat type could be directly recorded and sampled. More recently, Kettridge *et al*. (2008) used ground-penetrating radar (GPR) and complex electrical conductivity surveys complemented by hand coring to reveal horizontal zonation in peat geophysical properties to depths of *c*. 3 m along a 36-m transect in a raised bog in Maine in the USA. The observations made by Barber (1981) and Kettridge *et al*. (2008) may easily be verified by walking across a patterned bog: peat under hummocks is often firmer and safer to walk on than peat in lawns and hollows. However, such variations in structural strength may not necessarily translate into differences in hydrological properties such as water-storage capacity (e.g. specific yield or drainable porosity, *s*) and permeability or hydraulic conductivity (*K*).

Despite the recognition of lateral variability between microforms on bogs and an interest in how spatial patterns form (see below), there is little information on how hydrological properties vary between microforms. Some work has been done on poor fens (*sensu* Rydin & Jeglum 2006) which have similar types of vegetation to bogs. For example, in an undrained area of poor fen in Quebec, Canada, Whittington & Price (2006) found strong lateral variability in *K* of one-two orders of magnitude over distances of a few metres between a ridge (an elongated hummock or series of contiguous hummocks), a lawn and a 'mat', the latter a type of hollow. They also found that *K* declined by two to three orders of magnitude between depths of 0.25 and 1.25 m in these microforms, which is broadly what would be expected from the acrotelm-catotelm model. Therefore, lateral variability appears to be superimposed onto vertical variability. Whittington & Price's (2006) data are useful in showing that lateral variability can be substantial, but they only measured *K* at one location in one example of each microform, so their study lacked spatial replication. Ivanov (1981) reproduced empirical functions in which *K* at the same depth below the surface may vary by more than two orders of magnitude depending on microform type. However, it is not clear what data sets lie behind his functions (the number of measurements and sites from which the data behind the functions come are not listed) and they deal with shallow peat only

(upper ~ 0.4 m of peat profile). The latter issue – that of water flow in shallow *vs* deeper peat – is particularly pertinent, because, although he stressed the importance of lateral variation, Ivanov (1981) still considered shallow peat to be the main route for water flow, a key assumption of the acrotelm-catotelm model. There is abundant evidence that uppermost layers of bogs can be highly permeable (e.g. Boelter 1965; Hoag & Price 1995; Morris, Baird & Belyea 2015), but the situation with deeper peat is less clear. Some of the low *K* values reported for deeper peat may, in part, be measurement and sampling artefacts (see discussions in Koerselman (1989) and Baird, Surridge & Money (2004)). Where robust measurement protocols have been used there is evidence that deeper peat, on some sites at least, can be relatively permeable (e.g. Baird, Eades & Surridge 2008) and it is important that more work is done on estimating the *K* of deeper peat. Where permeable deeper peat is found, its effect on overall water flow through a bog will depend on whether it occurs in pockets isolated by poorly-permeable peat or whether it is connected to other higher-permeability zones (Belyea & Baird 2006). In other words, it is important to know both the absolute value of *K* and its spatial pattern – vertically and laterally – when considering the hydrological behaviour of bogs. The hydrological functioning of a peatland, often expressed in terms of the water-table regime, is closely linked with its ecological functioning (e.g. Belyea & Baird 2006; Roulet *et al*. 2007; Frolking *et al*. 2010; Morris, Baird & Belyea 2012), and anything that influences the behaviour of the water table will also affect key ecological processes such as litter production, vegetation composition, and depth-integrated rates of peat decay (e.g. Belyea & Clymo 2001).

A group of theoretical studies (Swanson & Grigal 1988; Couwenberg & Joosten 2006; Eppinga *et al*. 2009; Morris, Baird & Belyea 2013) used cellular landscape models to investigate the linkages between the hydrological and ecological functioning of peatlands, in particular how these linkages can lead to the development of hummock-hollow patterns. These models assume that the hydraulic properties of peat under different microforms are also different – they assume there is lateral variability – but also that most water flow occurs in the uppermost layers of a bog. Morris, Baird & Belyea (2013) showed that these models, despite considering horizontal variability, likely

lack some important ecohydrological feedbacks and may produce realistic patterns for the wrong reasons. Specifically, Morris, Baird & Belyea (2013) raised the question of whether microforms such as hummocks and hollows can be considered as features only of shallow peat, or whether their structural and hydrological importance at both the scale of the microform and the whole bog extends into deeper peat. They proposed a hypothetical mechanism for ecological memory (*sensu* Hendy & McGlade 1995) in peatlands whereby former surface vegetation patterns can leave a 3-dimensional imprint in the hydraulic structure of peat even after they are buried by litter from more recent plant assemblages. In a bog that possesses strong ecological memory of the type proposed by Morris, Baird & Belyea (2013), differences in peat properties (e.g. *K*) that characterise particular microform types would be evident not only near the surface in upper peat but also in deeper peat. Where a particular microform type had persisted for a long time, continued accretion would form a 3-dimensional pillar or curtain (*sensu* Belyea & Baird 2006) of peat that could be distinguished from adjacent peat produced by different microform types. In a bog with no ecological memory, deeper peat would be laterally homogenous in terms of the property of interest; i.e., even if microforms persisted in place for long periods, characteristic differences in the peat property of interest would only be identifiable in surficial layers and would not be preserved in deeper peat. A situation in which characteristic differences between microform types persist to a limited depth, or perhaps diminish gradually with depth, might be thought of as a weak ecological memory. It is clear that, to understand the patterning of peat hydrophysical properties in bogs, we must first understand how microforms develop and persist, and how peat properties change through time.

Materials and Methods

To address the first and second research questions on the magnitude and lateral variability of *K* in deeper peat, we measured *K* at two depths in two types of microform – ridges and hollows – in a Welsh raised bog. Measurements of the abundance of a range of plant macrofossils in cores of peat extracted from the bog were used to reconstruct the developmental history of the different

171 microforms used for the *K* measurements, thus providing data for answering the third research
172 question. The plant macrofossil and *K* data were complemented with measurements of peat dry bulk
173 density, degree of humification and age (from calibrated ^{14}C dates). Our combination of
174 palaeoecological techniques and detailed measurements of hydrological properties is perhaps an
175 unusual one, but serves as a powerful and novel tool for understanding ecohydrological memory in
176 peatlands.
177
178 *Field site and sampling rationale*
179 The site chosen for study – Cors Fochno in west Wales – has been described in detail in Baird,
180 Eades & Surridge (2008) and Kettridge *et al*. (2012). Its margins have been disturbed or damaged
181 by drainage and peat cutting, but its central area is undamaged and contains maze-like and
182 sometimes striped patterns of ridges, hummocks, lawns, and hollows that are typical of many raised
183 bogs and northern peatlands more generally (see Eppinga *et al*. 2009). Four microforms in this
184 central area were investigated: a ridge-hollow-ridge-hollow sequence at 52° 30' 10.0" N and 4° 00'
185 45.5" W. These features coincided with the first *c*. 10 m of the northern end of a 45-m transect used
186 by Kettridge *et al*. (2012) for a GPR survey of the peat, and are, for convenience, named Ridge 1,
187 Hollow 1, Ridge 2, and Hollow 2 (Fig. 1). Ridge vegetation comprised mostly *Calluna vulgaris*,
188 *Eriophorum vaginatum*, and *Sphagnum capillifolium*, with some *Eriophorum angustifolium* and
189 *Myrica gale*. Hollow vegetation was dominated by *Sphagnum pulchrum*, *Rhynchospora alba*,
190 *Eriophorum angustifolium*, with occasional *Erica tetralix* and *Myrica gale* plants (see Appendix
191 S1). The ground surface in the ridges was typically 0.05-0.10 m above that in the hollows (as
192 measured using an optical level – data not reported). The location of the ridges and their position
193 relative to the transect line used by Kettridge *et al*. (2012) is shown in Fig. 1.
194 We devised and conducted the study before the GPR data reported in Kettridge *et al*. (2012)
195 were analysed. GPR reflections from their survey tend to dip, and appear to indicate that
196 microforms at the site have migrated in one direction over time. However, the data obtained by

Kettridge *et al*. (2012) do not present a consistent picture. Dip angle decreases at depths of 1 m and less, suggesting that microform movement has slowed in the most recent period of bog development (last *c*. 1300 years according to data cited by Kettridge *et al*. (2012)). There are also sections along the 45-m transect (see Fig. 6c in Kettridge *et al*. (2012)) where the reflectors are flat, which suggests that some areas remain stable – their microforms do not move – while other areas, only a few metres away, are dynamic. Finally, for a 2.1-m section of the transect (27.4 m - 29.5 m) for which the GPR reflectors were dipping, detailed core analysis (eight cores at 0.30-m intervals) did not reveal any obvious dipping structures (Kettridge *et al*. 2012). As such it is unclear whether the microforms along our transect have been stationary or mobile through time. This issue relates directly to our third research question and we were able to determine if microforms had moved over time using our plant macrofossil and peat age data (see *Peat core collection and analysis* below).

*Hydraulic conductivity (*K*)*

To address the first and second research questions, *K* was measured in the four microforms using standpipe piezometers inserted into pre-augered holes. In each microform, five measurements were made at a nominal depth of 0.5 m and five at 0.9 m. These depths were chosen because they are below both the typical and the drought-year summer water table, and, therefore, represent what would usually be classified as the catotelm in the two-layer model (Ivanov 1981; Ingram 1983). Unpublished data from the site show that maximum water-table depths do not exceed 0.25-0.30 m in hollows and 0.40 m in ridges during summer drought. Separate locations were used for measuring *K* at the two depths. That is, we did not measure *K* at 0.5 m and then deepen the hole and measure *K* at 0.9 m; rather, we used separate holes, and these were at least 1 m distant from neighbouring holes. Therefore, we used a total of 40 locations for the *K* measurements. In this way we avoided a problem of repeated measures; each of our measurements could be regarded as independent at the scale of the microform.

Piezometer installation and *K* measurements followed the protocols presented by Baird, Surridge & Money (2004), Surridge, Baird & Heathwaite (2005), and Kelly *et al*. (2014). We used the same piezometer tubes as Surridge, Baird & Heathwaite (2005). These have an outside diameter (OD) of 0.033 m, an inside diameter (ID) of 0.029 m and 0.21 m long intakes. The centre of the intake was placed at each nominal depth – 0.5 m and 0.9 m.

Following installation, the piezometers were 'developed' or cleaned (Butler 1998; Baird, Surridge & Money 2004) to remove any smeared peat from around the intake. After development, a self-logging pressure transducer and a slug consisting of an acrylic rod were placed below the water level in each instrument. The water level was then allowed to stabilise before a head-recovery test was conducted by removing the slug. The removal of the slug caused the water level to fall by *c*. 0.04 m, and the subsequent rise in water level was recorded by the pressure transducer. Two types of pressure transducer were used – Mini-Diver and Micro-Diver units manufactured by Schlumberger Water Services (Delft, The Netherlands) – each with a resolution or precision of 0.002 m. A logging interval of 2 s was used for piezometers installed in the most permeable peat, while 4 s was used for slower-responding instruments. The shortest tests were completed within a few seconds; the longest took more than 12 hours (see below).

K was estimated from Hvorslev's (1951) equation:

$$K = -\frac{A}{Ft}\ln\left(\frac{h}{h_0}\right) \quad (1),$$

where A is the inside cross-sectional area of the piezometer standpipe (m^2), t is the time (s) at which the head difference, h (m) (see below), in the piezometer was recorded, h_0 is the initial head difference, and F is the shape factor (m) which is a function of the size and shape of the piezometer intake and the pattern of water flow around it (see Brand & Premchitt 1982). The head difference, h, is defined as the difference between the water level in the piezometer at any time during a head-recovery test and the water level prior to the withdrawal of the slug. h_0 is the difference at the moment the slug has been removed from the piezometer.

247 Strictly, equation (1) should only be applied to rigid media; peats are compressible and *K*
248 tests in them may not yield the log-linear recovery of the equation. However, it has been shown
249 (Baird & Gaffney 1994) that reliable estimates of *K* in peats may be obtained using the equation if
250 the head ratio (h/h_0) is close to zero; here, a value of $h/h_0 = 0.05$ and its associated time (t_{95}) were
251 used.
252 In some tests, the rate of water flow from the piezometer was so rapid that an initial head
253 difference could not be satisfactorily established. For these tests, it was assumed that t_{95} was 2 s. In
254 the 0.5-m tests carried out on Ridge 1, recovery was slow and coincided with a period of falling
255 heads in the peat around the piezometer intakes, making it difficult to estimate t_{95}. An example is
256 given in Fig. 2 which shows an apparent stalling of the head recovery. In these cases we assumed t_{95}
257 occurred at the turning point as shown by the arrow in the figure. This assumption will always give
258 a value of t_{95} that is too low, and therefore a value of *K* that is too high, compared to what would be
259 the case if background heads around the intake remained stable. Ideally, a period of stable heads
260 would have been used for the 0.5-m tests in Ridge 1. However, because recovery was so slow, it
261 would have been very difficult to find a time when heads remained stable for 12-24 hours; in most
262 bogs, heads often vary over such timescales due to gravitational water flow through the peat or
263 evaporative losses of water. Our assumed t_{95} values were, in any case, conservative because all of
264 the 0.5-m *K* estimates from Ridge 1 were lower than the lowest *K* recorded in any other feature at
265 either depth.
266 Hydraulic conductivity reflects both the properties of the porous medium and the liquid
267 flowing through it. As the viscosity of water changes with temperature so too does the hydraulic
268 conductivity. Our pressure transducers also measured temperature and we were able to use the
269 temperature data to convert our *K* values (as per Klute (1965)) to a standard temperature of 20°C.
270

Peat core collection and analysis

To reconstruct the developmental history of the microforms and to establish microform persistence (third research question), cores from each of the features were analysed for plant macrofossil remains, peat humification, and dry bulk density. In total, five cores were taken from each microform and each was 2 m in length. Three cores were taken from the centre of the microform (close to the intersection of the microform's long and short axes), each core being within 0.3 m of its two neighbours. One of these was analysed for peat decomposition or humification, one for dry bulk density (ρ_b), and one for plant macrofossils. Two additional 'humification cores', one from the western end and one from the eastern end of each feature (see Fig. 1) were also analysed. Plant fragments from the upper metre from two of the cores that were used for the macrofossil analysis – the cores from Ridge 2 and Hollow 2 – were ^{14}C dated (dates calibrated using IntCal09 – see below), and six dates from three depths in each core were obtained. All of the cores were taken with a Russian corer, with a semi-circular chamber with a diameter of 0.038 m.

Peat humification, an indicator of the degree of decomposition, was estimated visually from fresh peat in the field. The color and texture of the peat in the core were used to define peat layers, and each layer was classified using the von Post humification scale from H1 (completely undecomposed) to H10 (completely decomposed) (see Rydin & Jeglum 2006). The humification estimates were conducted by the same person (A.M.M.) for all cores, and the von Post descriptions given in Rydin & Jeglum (2006, p. 86) were used as a constant reference to ensure consistency in classification.

In the bulk density cores, samples were taken, where possible, from 0-0.02 m, 0.10-0.12 m, 0.20-0.22 m and so on below the surface. Poor recovery in parts of the cores meant that not all the required depths could be sampled. Seventeen samples were recovered from Hollow 1, six from Hollow 2, 18 from Ridge 1 and 19 from Ridge 2. The samples were placed in foil sachets in the field and then wrapped in clingfilm for later analysis. They were stored in a cold room below 4 °C upon return to the laboratory. After removal from storage, they were dried at 80 °C for 24 hours

297 before being cooled in a desiccator and weighed. The samples were not ashed, so the values of ρ_b
298 that were calculated were not corrected for the presence of any non-organic material.
299 Each of the four macrofossil cores was divided into bulked samples for each 0.1-m depth
300 interval. Thus, samples represented depths of 0-0.1 m, 0.1-0.2 m and so on, with each sample
301 having a volume of *c*. 5.7×10^{-5} m^3 depending on core recovery. It is unusual to use bulked cores
302 like this for plant macrofossil analysis. More typically, samples that span a 0.01-m depth range are
303 analysed. Sometimes these are contiguous, but, because they are time-consuming to analyse, they
304 are often spaced at intervals of 0.02-0.08 m (Amesbury, Barber & Hughes 2010). The problem with
305 the latter is that critical information may be lost. For example, there may have been a switch
306 between vegetation types in the un-analysed zone between two 0.01-m samples; in effect, the record
307 is incomplete, even though the information from a 0.01-m layer can be ascribed accurately to a
308 particular depth and date. There is inevitably some loss of information and resolution with our
309 method, but it guarantees that all plant types present within a 0.1-m length of core are recorded,
310 including their abundance, making it possible to establish if there have been switches between
311 vegetation types during the time period represented by the 0.1 m.
312 Each macrofossil sample (i.e., the entire 5.7×10^{-5} m^3) was prepared for examination using
313 standard techniques as detailed by Barber *et al*. (1994). Macrofossil examination followed the
314 Quadrat and Leaf Count Method (Barber *et al*. 1994) but with some modifications as described
315 below. Before examination, each prepared sample was mixed thoroughly and emptied into a large-
316 diameter (0.15 m) Petri dish. A low-powered microscope fitted with a 10 × 10 square grid (quadrat)
317 in the eyepiece allowed percentage coverage of different macrofossil components to be estimated.
318 When possible, 100 *Sphagnum* leaves were picked from the sample, mounted on slides, examined at
319 × 100-400 magnification and identified to species or at least section level. Differentiation between
320 monocotyledon remains was also achieved when suitable epidermal tissue was found (Mauquoy,
321 Hughes & van Geel 2010). Five quadrat estimations were completed for each sample. Seeds,
322 ericaceous leaves and charcoal were counted separately.

We obtained six accelerator mass spectrometry (AMS) ^{14}C dates of the peat in the study area, three from Hollow 2 and three from Ridge 2 (Fig. 1). Plant fragments for dating were obtained from depths of 0.2-0.3 m, 0.5-0.6 m, and 0.9-1.0 m from the two cores used for the plant macrofossil analysis (see above). The mixed samples of peat from the 0.1-m intervals (see above) were washed with deionised water in a 125 µm sieve, and, in order to minimise potential contamination, *Sphagnum* leaves, branches, and stems were used for the dating, except for the 0.9-1.0 m interval in Ridge 2 where we used *Racomitrium lanuginosum* leaves and stems. Care was taken to remove ericaceous roots to prevent any possible reservoir effects as described by Kilian, van der Plicht & van Geel (1995). The plant fragments were dated at the ^{14}CHRONO Centre at Queen's University, Belfast (an acid-alkali-acid pre-treatment was used). The ^{14}C dates were calibrated using IntCal09 (Reimer *et al*. 2009).

Data analysis

Except for those piezometers noted earlier where an initial head difference could not be established or where recovery stalled, we estimated t_{95} as the first reading where $h/h_0 \leq 0.05$. We conducted repeat *K* tests on some piezometers to help gauge within-instrument test variability and these showed similar consistency to previous studies (see Appendix S2 in Supporting Information). As well as differences in *K* between microform type (ridge, hollow) and depth, we were interested in all comparisons across the *K* data set to see whether differences between, say, ridges and hollows depends on which ridge and which hollow are being considered. We used a Bayesian multiple pair wise comparison developed by Kruschke (2011; chapter 18) that allows for non-homogenous variance between groups, a group being, for example, all the readings at 0.5 m in Hollow 1. We undertook the analysis on the $\log_e$ transformed data. In the Bayesian analysis, the data as a whole (combined from all groups) are standardised to have a mean of zero and a standard deviation of 1. The model describing the standardised data is given by:

$$u_i = \beta_0 + \sum_j \beta_j x_{ji} \quad (2)$$

where u_i is the mean of the distribution of individual values (y_i), β_0 is a baseline value of u_i, while β_j is the deflection from β_0 for group j. x may take values of 0 or 1. β_0 is described by a normal distribution with a mean of zero and a precision of 0.001 (variance of 1000). β_j is also described by a normal distribution, which has a mean of zero and a precision specified by a folded t distribution with a mean of zero, a precision of 0.001 and a k or shape setting of 2. These priors for the models of both β_0 and β_j are highly non-committal and have a very small influence on the posterior (or outcome) of the Bayesian analysis. To account for unequal variance between groups, the precision of the distribution of y_i is estimated separately for each group from a gamma distribution (see Kruschke 2011).

The Bayesian method was applied using the data and multiple random sampling from the data models as specified with the non-committal priors. Sampling was performed using a Markov Chain Monte Carlo (MCMC) process (Kruschke 2011) with a sample size of 100 000 after a 'burn-in' of 5000 steps. The pair-wise analysis was carried out using R and JAGS (R Core Team 2012) and the code and its source are given in Appendix S3. The MCMC analysis yields distributions of differences in β_j for each pair of groups. In these distributions we may define a highest density interval or HDI in which 95% of the difference values lie. If the HDI does not include zero we may conclude that there is a credible difference in K between the groups.

To assess whether there is evidence of the persistence of each of the microforms over the period of time represented by the 2 m peat cores, we applied cluster analysis with multiple bootstrap resampling to the plant macrofossil biostratigraphic data. This analysis enables the calculation of *p*-values to identify statistically significant clusters (Suzuki & Shimodaira 2006) and was used to determine the similarity-dissimilarity of samples between the hollow and ridge cores. We also undertook nonmetric multidimensional scaling (NMDS; Minchin 1987) using the Bray-Curtis dissimilarity index to examine the main axes of variation in the plant macrofossil data. The Bray-Curtis dissimilarity index is a popular and effective index for ecological data and is defined as:

$$d^{BCD}(i,j) = \frac{\sum_{k=0}^{n-1} \left| y_{i,k} - y_{j,k} \right|}{\sum_{k=0}^{n-1} \left(y_{i,k} - y_{j,k} \right)} \quad (3)$$

where d^{BCD} is the Bray-Curtis dissimilarity between the objects *i* and *j*, *k* is the index of a variable and *n* is the total number of variables *y* (e.g. Legendre & Legendre 1998). The stress was analysed in several runs to ensure a robust result was achieved. Ordination 'spiders' were used to demarcate the four microforms and assess similarity/dissimilarity. The analysis was carried out using the vegan package (v. 2.0-5) in R (v. 2.15.1) (Oksanen *et al*. 2012; R Core Team 2012).

It is common in plant macrofossil analysis to include Ericaceae as a class and we followed this convention when compiling our data (see **Results**; *Macrofossils, humification and bulk density*). However, Ericaceae was left out of the cluster and NMDS analysis because its main components – *Calluna vulgaris* and *Erica tetralix* – may, between them, occupy a range of wetness conditions from hollow to ridge. *Calluna vulgaris* is usually a reliable dry or ridge indicator. However, although *Erica tetralix* is often used by palaeoecologists as a dry indicator (e.g. Mauquoy *et al*. 2008), it is more flood-tolerant than *Calluna vulgaris* (e.g. Bannister 1964) and, unlike the latter, may be common in wet conditions such as the fringe of bog pools (Elkington *et al*. 2001). Rare taxa (with maximum values of 4% or less) were also excluded from the NMDS analysis.

Age-depth models for Ridge 2 and Hollow 2 were constructed using the 'Bacon' piece-wise linear accumulation model of Blaauw & Christen (2011) in R (R Core Team, 2012). In this model, the accumulation rate of sections depends to a degree on that of neighbouring sections, accumulation rates are constrained by a prior distribution (a gamma distribution with parameters acc.mean and acc.shape), as is the variability in accumulation rate between neighbouring depths ('memory', a beta distribution with parameters mem.mean and mem.strength). In our analysis, 0.05 m-thick sections were used along with acc.shape = 2 and acc.mean = 13 yr cm^{-1}. The prior information was combined with the radiocarbon dates and a 2011 date for the peat surface using millions of MCMC iterations (Blaauw & Christen 2011). The total chronological error (difference

between maximum and minimum probability ages at 95 %) associated with each depth was calculated from the model. Ages for the 0.1 m-thick dating samples were defined using the Bacon model and expressed in histograms (see Appendix S4).

Results

Hydraulic conductivity

The hydraulic conductivity (*K*) data are summarised in Fig. 3, with the data separated according to microform and depth. The data show that *K* varies by nearly four orders of magnitude across the site. The highest *K* values were more than 1×10^{-3} m s^{-1} while the lowest values were less than 1×10^{-6} m s^{-1}, equivalent, respectively, to the *K* of a coarse sand and that of a silt (Domenico & Schwartz 1990). The data also suggest that there are differences in *K* between microforms. For depths of 0.5 m, hollow *K* appears to be significantly higher than ridge *K*, with nine of the 10 hollow values exceeding the highest value from the ridges. Four of the 10 hollow values exceed the highest ridge value by at least an order of magnitude and two of the 10 exceed the highest ridge value by a factor of *c*. 250. At a depth of 0.9 m, the differences between features are less clear. All of the values from Hollow 1 exceed all of the values from Ridges 1 and 2. However, there is an overlap between the values from Hollow 2 and both ridges. The data also suggest that there are differences in the *K* values between microforms of the same type and the same depth. For example, at 0.5 m depth, all of the *K* values from Ridge 2 are higher than those from Ridge 1. Similarly, all of the *K* values at a depth of 0.9 m in Hollow 1 are higher than the values at the same depth in Hollow 2.

The results from the Bayesian analysis are summarised in Table 1 and given in more detail in Appendix S3. Table 1 identifies those categories in which the highest density interval (HDI) of between-group differences in the deflections – β_j – does not include zero; as noted above (see **Materials and Methods**; *Data analysis*) this may be thought of as indicating a credible difference

between a pair of groups based on the data that have been collected. In terms of between-group differences, the most interesting features from the Bayesian analysis are as follows.

Depths of 0.5 m. Ridge 1 is credibly different from all other groups at this depth (Ridge 2, and Hollows 1 and 2). Ridge 2 also differs from Hollows 1 and 2; therefore, despite the difference between Ridge 1 and Ridge 2, there is credible evidence that the ridges at 0.5 m are different from the hollows at the same depth.

Depths of 0.9 m. Hollow 1 is credibly different from both ridges at this depth. Hollow 2, however, is not credibly different from either ridge. These results contrast with those from 0.5 m where ridges and hollows show clear differences; at 0.9 m there is no such pattern in the data. Notably, Ridges 1 and 2 show no credible difference at this depth, unlike at 0.5 m.

The pairwise comparisons also suggest that there is a credible difference between depths in Ridge 1, but not in the other three microforms, although in Hollow 2 the HDI in the contrast between 0.5 m and 0.9 m only just straddles zero (Table 1), so there is some suggestion of a real difference in *K* values between depths. In Ridge 1 the 0.5-m or younger peat has a lower *K* than the deeper peat, while in Hollow 2 the opposite is the case.

Peat age-depth profiles

Radiocarbon dates of the extracted plant fragments from Hollow 2 and Ridge 2 are given in Table 2. The age-depth models that were derived from the data are given in Appendix S4. Age-depth curves for each feature are given in Fig. 4. These show different trajectories for each feature. For 1 m in Ridge 2 the modelled age is 1520-1330 cal. BP (mean = 1390 cal. BP) whereas for 1 m in Hollow 2 the modelled age is 1315-1080 cal. BP (mean = 1180 cal. BP).

The peat accumulation rates for Ridge 2 and Hollow 2 show variations. For Ridge 2 the accumulation rate was higher in the lower part of the core and decreased towards the top of the core (*c*. 0.11 cm yr^{-1} from 0.57-1.00 m depth, compared with 0.05 cm yr^{-1} from 0.00-0.57 m depth). For Hollow 2, the accumulation rates were more mixed, with lower and less variable rates in the lower

449 part of the core (*c*. 0.07 cm yr^{-1} from 0.57-1.00 m) and higher and more variable rates in the upper
450 part. The maximum and minimum accumulation rates were similar, with maxima of 0.14 and 0.15
451 cm yr^{-1} for Ridge 2 and Hollow 2, respectively, and a minimum of 0.05 cm yr^{-1} for both features.
452 These interpretations are somewhat tentative due to the relatively low number of radiocarbon dates.
453
454 *Macrofossils, humification and bulk density*
455 The macrofossil, humification and dry bulk density data for the three separate cores taken from the
456 centre of each microform are shown in Figs 5a and 5b. The data from the additional humification
457 cores (two per microform) are available in Appendix S5.
458 The four microforms differ in their peat profiles in terms of degree of decomposition,
459 macrofossil composition and abundance, and dry bulk density. Taxa indicative of surface wetness
460 (water tables close to the surface) are more abundant in the two hollow cores (Fig. 5a) than in the
461 two ridge cores (Fig. 5b), and *vice versa*. For example, ridge cores are notably characterised by
462 *Sphagnum austinii*, while hollow cores are dominated by *Sphagnum* section Cuspidata,
463 *Rhynchospora alba* and *Sphagnum papillosum* with occasional abundance of monocotyledons and
464 *Menyanthes trifoliata*. However, 'wetter' taxa are evident, and sometimes common, in the ridge
465 cores and drier taxa in the hollow cores.
466 Our analysis revealed a number of statistically significant clusters ($p < 0.05$) (Fig. 6), and
467 shows, generally, that the ridges and hollows are strongly differentiated from each other; Hollow 1
468 is most similar to Hollow 2, and Ridge 1 is most similar to Ridge 2. However, while Ridge 2 and
469 Hollow 2 are mostly distinct features, there is considerable overlap between Ridge 1 and Hollow 1.
470 The NMDS analysis of the macrofossil data shown in Fig. 7 gives a similar outcome to the cluster
471 analysis. The major gradient in the dataset (NMDS axis 1; Fig. 7) follows a ridge-hollow/bog
472 surface wetness gradient. It is apparent that Ridge 2 and Hollow 2 are separate from each other in
473 the ordination space, whereas Hollow 1 and Ridge 1 overlap; the axis 1 scores illustrate this
474 separation and overlap clearly. The analysis confirms what appears to be evident from the

475 macrofossil diagrams: Ridge 2 and Hollow 2 have consistently been a ridge and hollow,
476 respectively, throughout their developmental history as represented by their respective macrofossil
477 NMDS axis 1 scores. The cores from Hollow 1 and Ridge 1 have a more mixed signal in terms of
478 macrofossils although Hollow 1 is more hollow-like than Ridge 1, and Ridge 1 is more ridge-like
479 than Hollow 1.

480 Generally, the two ridge cores have more decomposed peat than the two hollow cores: the
481 average humification from the Ridge 1 and 2 cores is H7 and H8, respectively (Ridge 1, n = 44;
482 Ridge 2, n = 53), whereas the average humification for the Hollow 1 and 2 cores is H6 (Hollow 1, n
483 = 60; Hollow 2, n = 48). However, there is considerable down-core variability in humification in all
484 cores (see Appendix S5).

485 The dry bulk density (ρ_b) for all the microforms was below 100 kg m^{-3} and ranges from 21
486 to 86 kg m^{-3} (Figs 5a and 5b). The highest ρ_b values were recorded in Ridge 2, and the lowest in
487 Hollow 1. The average ρ_b for Hollows 1 and 2 is, respectively, 35 kg m^{-3} (n = 17) and 33 kg m^{-3} (n =
488 6 due to poor core recovery); the averages for Ridge 1 and 2 are 45 kg m^{-3} (n = 18) and 60 kg m^{-3} (n
489 = 19). The ρ_b values for Ridge 1 and 2 show little overlap with the values of Hollow 1 and 2: the
490 ridges have consistently higher ρ_b than the hollows.

491

492 **Discussion**

493 *High* K *in deeper peat*

494 From an ecohydrological perspective the first two research questions on the magnitude and lateral
495 variability of deeper-peat K only assume importance if the permeability of the deeper peat is
496 sufficiently high to allow non-trivial rates of water flow. Even if there is an order of magnitude
497 difference in the K of the deeper peat between hollows and ridges, the difference may be
498 unimportant if those K values are low: for example, water flow through peat with a permeability in
499 the range of 1-10 $\times$ 10^{-9} m s^{-1} will be negligible under natural hydraulic gradients, so it does not
500 matter if different microform types lie at opposite ends of this range.

In the two-layer acrotelm-catotelm model, the acrotelm conducts the vast majority of water, with largely stagnant conditions prevailing in the catotelm because of its low *K*. While we found that deeper-peat (catotelm) *K* can be low and consistent with the model, such as in Ridge 1 at a nominal depth of 0.5 m (Fig. 3), we also found that *K* in deeper peat could equal and exceed values for shallow, near-surface, peat at the site (Fig. 3) and for a range of other peatlands – see, for example, Boelter (1965), Hoag & Price (1995), Quinton, Hayashi & Carey (2008), Lewis *et al*. (2012), and Morris, Baird & Belyea (2015) (Fig. 3). In each of these studies, *Sphagnum* was often the main or an important peat-forming species, and the highest *K* values reported in each were generally associated with the least decomposed peat. Our results show that deeper bog peat has the potential to conduct non-trivial amounts of water; as such, our data are inconsistent with one of the principal features of the two-layer model. This finding adds weight to the growing argument (Holden & Burt 2003; Morris *et al*. 2011) that the two-layered model is too rigid a framework to be generally applicable, because the intricacies of peatland ecohydrological structures and functions do not necessarily partition neatly into two catch-all layers. However, whether the *K* values we observed in deeper peat layers actually lead to rapid flows will depend on the connectivity of zones of high *K* within the deeper peat, and more work is required on mapping subsurface structures at the site.

Microform persistence and K *variations*

Based on the age-depth model, Hollow 2 has persisted since at least *c*. 1200 cal BP and Ridge 2 since at least *c*.1400 cal BP. Because they extend to twice the depth of the deepest dated samples, the macrofossil data show that both microforms have persisted for considerably longer than these ages. Both features are, therefore, ancient, persisting as the bog increased markedly in vertical extent. The other two microforms – Hollow 1 and Ridge 1 – show a mixed signal; they have undergone switches in their status over time. Nevertheless, Hollow 1 has been more hollow-like than ridge-like throughout its development, and Ridge 1 has been more ridge-like than hollow-like.

Therefore, there is little evidence to support the suggestion of uni-directional microform movement at the site. This finding is not necessarily inconsistent with what is suggested in Kettridge *et al*. (2012) who found that dipping reflectors indicative of microform movement were more steeply sloping in the peat at depths of 1-2.5 m than shallower depths; in other words that the evidence of microform movement in the uppermost metre of peat is less strong than the evidence from the deeper peat. Nevertheless, based on their GPR data, current microform spacing and an age-depth model constructed from data from Schulz (2004), Kettridge *et al*. (2012) suggested that a microform passing a fixed point would be expected to produce layers of peat with a mean thickness of *c*. 0.19 m. When superimposed on such layers, our contiguous 0.1-m samples should consist of some in which there is a hollow-only signal, some which are ridge-only, and some that contain a mixture of wet and dry indicators. Such a pattern of both pure and within-sample mixed signals is not evident in the data from Hollow 2 and Ridge 2, which contain, respectively, hollow-like and ridge-like properties throughout most of their profiles. In Hollow 1 and Ridge 1, there is evidence of switches in microform type but these don't conform to the pattern expected from 0.19-m layers, regardless of how a 0.1-m sampling interval is staggered. Therefore, the switches seen in Hollow 1 and Ridge 1 are more likely to be due to microform contraction/expansion as per the conceptual model of Aaby (1976) and Barber (1981). Whether such contraction/expansion resulted from climatic changes remains unclear (it may be autogenic or allogenic).

Multivariate statistical tools such as the cluster analysis and NMDS we apply here provide an objective statistical approach for classifying microforms and assessing how distinct they have been through their developmental history. NMDS enables the determination of whether plant assemblages in each microform have remained consistent, or whether switches in the microform characteristics have occurred. We contend that using robust statistical tools such as NMDS is less prone to bias than traditional approaches where stratigraphic data are zoned and classified by eye.

Peat formed in ridges (from ridge vegetation) is different, botanically, from that formed in hollows (from hollow vegetation), and the plant macrofossil data suggest that Hollow 2 has been

553 more hollow-like than Hollow 1 throughout its history and Ridge 2 has been more ridge like than
554 Ridge 1. With this in mind, we might expect the *K* at 0.5 m and the *K* at 0.9 m – $K_{0.5}$ and $K_{0.9}$ – to
555 show the greatest differences between Hollow 2 and Ridge 2, but this is not the case. The difference
556 in $K_{0.5}$ between Hollow 1 and Ridge 1 is much greater than that between Hollow 2 and Ridge 2,
557 while for $K_{0.9}$ the Bayesian analysis suggest that there is no credible difference between Hollow 2
558 and Ridge 2 although there is one between Hollow 1 and Ridge 1 (Fig. 3; Table 1; Appendix S3).
559 These differences may be taken to suggest that ecological memory is relatively weak at the site; i.e.,
560 although Hollow 2 and Ridge 2 have persisted over time – considerably longer than *c*. 1200 and
561 1400 years – this persistence is not reflected in their *K* values. Such a conclusion might be
562 premature because Hollow 2 and Ridge 2 are credibly different in terms of their $K_{0.5}$ values. Also,
563 more generally, both ridges at 0.5 m separate clearly from hollows at the same depth, with higher *K*
564 values in the hollows. It is notable that such a clear separation does not occur at 0.9 m, which may
565 indicate a weakening of ecological memory with time. What is clear is that our data do not provide
566 a simple answer to the third research question; patterns in *K* are not easily attributable to microform
567 persistence and ecological memory.

568 The strong horizontal contrasts in $K_{0.5}$ are almost as striking as those that can occur
569 vertically within the upper *c*. 0.2-0.5 m of the peat profile ('acrotelm'). For example, median $K_{0.5}$
570 varies by two orders of magnitude between Ridge 1 and the adjacent Hollow 1, and by an order of
571 magnitude between Ridge 2 and its Hollow 2 neighbour (Fig. 3). Such strong horizontal gradients in
572 *K* are further indication that our study site is not well described by the acrotelm-catotelm model,
573 which is unable to account for horizontal variations.

574 Although there are patterns in the *K* data, it is important to recognise that deeper-peat *K*
575 values may not fit neatly into simple categories or always correspond in a simple way to peat type
576 (botanical composition and degree of decomposition). Care has to be taken to avoid over-
577 interpreting the plant-macrofossil data from the central core of each of the studied microforms
578 because the data from these cores may not apply to each piezometer location (the piezometers for

579 the *K* tests were located across each feature). Nevertheless, if incursions of the 'other' peat type
580 (hollow peat in a 'ridge' and ridge peat in a 'hollow') occur in the centre of a feature, they should
581 also occur across the rest of the feature where the piezometers were placed. Therefore, if an
582 incursion recorded by the centrally-located macrofossil core corresponds to the depth at which *K*
583 was measured, we can consider more closely how peat type affects *K*. If we look in detail at Ridge
584 1, for example, at the depth interval of *c*. 0.4-0.6 m (the range over which $K_{0.5}$ was measured) there
585 is a hollow-like incursion: there are peaks in the abundance of *Sphagnum* section Cuspidata,
586 *Sphagnum papillosum*, and *Menyanthes trifoliata* (Fig. 5b). The von Post score over this range
587 shows a moderate degree of decomposition (H4), and ρ_b varies between *c*. 45 and *c*. 55 kg m^{-3}.
588 Despite such conditions, the $K_{0.5}$ values recorded for Ridge 1 were the lowest five from the 40-
589 strong data set. In contrast, $K_{0.5}$ was very high in Hollow 1 for a very similar plant macrofossil
590 signal and a higher von Post score (H4-H7), although ρ_b was lower (30-45 kg m^{-3}) (Fig. 3 and Fig.
591 5a). Finally, and in a similar vein, the very high $K_{0.9}$ values recorded from Hollow 1 coincide with a
592 peak in *Sphagnum austinii*, indicative of hummock or ridge-like conditions, relatively high von Post
593 scores (H5-H7), but low ρ_b values (below 30 kg m^{-3}).

594 Why do such apparent anomalies occur? The *K* of a porous medium is very sensitive to the
595 pore size distribution, so one modest sized pore can conduct more water than multiple small pores
596 with a combined cross-sectional area many times that of the single pore. This sensitivity to pore size
597 or diameter is an outcome of the capillary bundle analogy and Poiseuille's law (Dingman 1984). A
598 soil such as peat may be considered analogous to a bundle of capillary tubes. In each tube, flow is
599 laminar and follows Poiseuille's law; it increases with the fourth power of pore diameter. Given the
600 sensitivity of water flow, and therefore permeability, to one or two macropores, it is perhaps
601 unsurprising that *K* does not always vary simply with peat or microform type.

602 Our data were collected from a small number of microforms and, arguably, stronger patterns
603 might emerge were a larger study to be done, or many similar studies were done across a range of
604 sites. We encourage other researchers to take up this challenge; if the work is extended, we will be

in stronger position to understand the importance of peatland microforms to overall peatland functioning and to parameterise peatland models more accurately.

While our results indicate clear patterns in *K* between adjacent hummocks and hollows at 0.5 m depth, the picture is less clear at 0.9 m; the evidence for characteristic hydraulic structures associated with hummocks and hollows extending beyond the uppermost peat is mixed and it would be premature to assume that deeper-peat *K* differs in any consistent or predictable manner between microforms. As such, evidence for the mechanism for ecological memory in peatlands proposed by Morris, Baird & Belyea (2013) is similarly mixed. Our results indicate that while such an effect may exist, it is likely to diminish with depth and age as old peat layers become buried by younger peat.

We find that some peatland microforms may persist over millennial timescales (Hollow 2 and Ridge 2), while other, proximal, microforms are characterised by switches between wet and drier conditions (Hollow 1 and Ridge 1). We suggest that such switches are more likely to be contraction/expansion in line with the conceptual model of Aaby (1976) and Barber (1981) rather than the spatial migration of individual microforms. There is debate over whether such switches can be purely autogenic in nature, or if they correspond to climatic shifts. Our findings have important implications for understanding the functioning of peatlands – even over short distances there can be marked heterogeneity in terms of developmental history and ecohydrological dynamics.

Acknowledgements

We thank Nikki Dodd from the James Hutton Institute, Aberdeen, Scotland, for taking the aerial photograph of the field site used in Fig. 1. This work was funded by The University of Leeds and the private funds of A.J.B. and A.M.M. Natural Resources Wales (formerly the Countryside Council for Wales) and Mike Bailey are thanked for giving permission to work on the site. We are grateful to Professor Henry Lamb from the University of Aberystwyth for the loan of his Russian

corer. Finally, we thank the reviewers – one anonymous and the other Professor Nigel Roulet – whose comments helped us greatly improve the manuscript.

Data accessibility

The permeability and palaeo-ecological data (including dry bulk density and degree of humification) are available in the Dryad Digital Repository (Baird *et al*. 2015): http://dx.doi.org/10.5061/dryad. v5r86.

The R script for the Bayesian pair-wise analysis is available as online supporting information.

References

Aaby, B. (1976) Cyclic climatic variations in climate over the past 5,500 yr reflected in raised bogs. *Nature*, **263**, 281-284.

Amesbury, M.J., Barber, K.E. & Hughes, P.D.M. (2010) The methodological basis for fine-resolution, multiproxy reconstructions of ombrotrophic peat bog surface wetness. *Boreas*, **40**, 161-174.

Baird, A.J., Belyea, L. & Morris, P.J. (2009) Upscaling peatland-atmosphere fluxes of carbon gases: small-scale heterogeneity in process rates and the pitfalls of 'bucket-and-slab' models. *Carbon Cycling in Northern Peatlands* (eds A.J. Baird, L.R. Belyea, X. Comas, A. Reeve & L. Slater), pp. 37-53. Geophysical Monograph Series 184, American Geophysical Union, Washington, DC.

Baird, A.J. & Gaffney, S.W. (1994) Cylindrical piezometer responses in a humified fen peat. *Nordic Hydrology*, **25**, 167-182.

Baird, A.J., Eades, P.A. & Surridge, B.W.J. (2008) The hydraulic structure of a raised bog and its implications for ecohydrological modelling of bog development. *Ecohydrology*, **1**, 289-298.

655 Baird, A., Milner, A., Blundell, A., Swindles, G. & Morris, P. (2015) Data from: Microform-scale
656 variations in peatland permeability and their ecohydrological implications. *Dryad Digital*
657 *Repository*, http://dx.doi.org/10.5061/dryad. v5r86.
658 Baird, A.J., Surridge, B.W.J. & Money, R.P. (2004) An assessment of the piezometer method for
659 measuring the hydraulic conductivity of a *Cladium mariscus-Phragmites australis* root mat
660 in a Norfolk (UK) fen. *Hydrological Processes*, **18**, 275-291.
661 Bannister, P. (1964) The water relations of certain heath plants with reference to their ecological
662 amplitude. III. Experimental studies: General conclusions. *Journal of Ecology*, **52**, 499-509.
663 Barber, K.E. (1981) *Peat Stratigraphy and Climatic Change: A Palaeoecological Test of the Theory*
664 *of Cyclic Peat Bog Regeneration*. A.A. Balkema, Rotterdam.
665 Barber, K.E., Chambers, F.M., Maddy, D., Stoneman, R. & Brew, J.S. (1994) A sensitive high-
666 resolution record of Late Holocene climatic change from a raised bog in northern England.
667 *The Holocene*, **4**, 198-205.
668 Belyea, L.R. & Baird, A.J. (2006) Beyond the "limits to peat bog growth": cross-scale feedback in
669 peatland development. *Ecological Monographs*, **76**, 299-322.
670 Belyea, L.R. & Clymo, R.S. (2001) Feedback control of the rate of peat formation. *Proceedings of*
671 *the Royal Society of London Series B – Biological Sciences*, **268**, 1315-1321.
672 Blaauw, M. & Christen, J.A. (2011) Flexible paleoclimate age-depth models using an
673 autoregressive gamma process. *Bayesian Analysis*, **6**, 457-474.
674 Boelter, D.H. (1965) Hydraulic conductivity of peats. *Soil Science*, **100**, 227-230.
675 Brand, E.W. & Premchitt J. (1982) Response characteristics of cylindrical piezometers.
676 *Géotechnique*, **32**, 203-216.
677 Butler, J.J. Jr. (1998) *The Design, Performance and Analysis of Slug Tests*. Lewis Publishers, Boca
678 Raton, Florida.
679 Couwenberg, J. & Joosten, H. (2006) Self-organization in raised bog patterning: the origin of
680 microtope zonation and mesotope diversity. *Journal of Ecology*, **93**, 1238-1248.

681 Dingman, S.L. (1984) *Fluvial Hydrology*. W.H. Freeman, New York.
682 Domenico, P.A. & Schwartz, F.W. (1990) *Physical and Chemical Hydrogeology*. Wiley, New
683 York.
684 Elkington, T., Dayton, N., Jackson, D.L. & Strachan, I.M. (2001) *National Vegetation*
685 *Classification: Field Guide to Mires and Heaths*. Joint Nature Conservation Committee,
686 Peterborough, UK.
687 Eppinga, M.B., de Ruiter, P.C., Wassen, M.J. & Rietkerk, M. (2009) Nutrients and hydrology
688 indicate the driving mechanisms of peatland surface patterning. *American Naturalist*, **173**,
689 803-818.
690 Frolking, S., Roulet, N.T., Tuittila, E., Bubier, J.L., Quillet, A., Talbot, J. & Richard, P.J.H. (2010)
691 A new model of Holocene peatland net primary production, decomposition, water balance,
692 and peat accumulation. *Earth System Dynamics*, **1**, 1-21.
693 Hendry, R.J. & McGlade, J.M. (1995) The role of memory in ecological systems. *Proceedings of*
694 *the Royal Society of London Series B – Biological Sciences*, **259**, 153-159.
695 Hoag, R.S. & Price, J.S. (1995) A field-scale, natural gradient solute transport experiment in peat at
696 a Newfoundland blanket bog. *Journal of Hydrology*, **172**, 171-184.
697 Holden, J. & Burt, T.P. (2003) Hydrological studies on blanket peat: the significance of the
698 acrotelm-catotelm model. *Journal of Ecology*, **91**, 86-102.
699 Hvorslev, M.J. 1951. *Time Lag and Soil Permeability in Groundwater Observations*. Waterways
700 Experimental Station Bulletin 36, United States Army Corps of Engineers, Mississippi,
701 USA.
702 Ingram, H.A.P. (1978) Soil layers in mires: function and terminology. *Journal of Soil Science*, **29**,
703 224-227.
704 Ingram, H.A.P. (1983) Hydrology. *Mires: Swamp, Bog, Fen and Moor* (ed. A.J.P. Gore), pp. 67-
705 158, Elsevier, Amsterdam.
706 Ivanov, K.E. (1953) *Gidrologiya Bolot* [Hydrology of Mires]. Gidrometeoizdat, Leningrad.

707 Ivanov, K.E. (1981) *Water Movement in Mirelands*. English language edition translated by
708 Thompson, A. & Ingram, H.A.P., Academic Press, London.
709 Kelly, T.J., Baird, A.J., Roucoux, K.H., Baker, T.R., Honorio Coronado, E.N., Ríos, M. & Lawson,
710 I.T. (2014) The high hydraulic conductivity of three wooded tropical peat swamps in
711 northeast Peru: measurements and implications for hydrological function. *Hydrological*
712 *Processes*, **28**, 3373-3387.
713 Kettridge, N., Binley, A., Comas, X, Cassidy, N.J., Baird, A.J., Harris, A., van der Kruk, J., Strack,
714 M., Milner, A.M. & Waddington, J.M. (2012) Do peatland microforms move through time?
715 Examining the developmental history of a patterned peatland using ground penetrating
716 radar. *Journal of Geophysical Research – Biogeosciences*, **117**, G03030.
717 Kettridge, N., Comas, X., Baird, A., Slater, L., Strack, M., Thompson, D., Jol, H. & Binley, A.
718 (2008) Ecohydrologically-important subsurface structures in peatlands are revealed by
719 ground-penetrating radar and complex conductivity survey. *Journal of Geophysical*
720 *Research – Biogeosciences*, **113**, G04030.
721 Kilian, M.R., van der Plicht, J. & van Geel, B. (1995) Dating raised bogs: new aspects of AMS ^{14}C
722 wiggle matching, a reservoir effect and climatic change. *Quaternary Science Reviews*, **14**,
723 959-966.
724 Klute, A. (1965) Laboratory measurement of hydraulic conductivity of saturated soil. *Methods of*
725 *Soil Analysis. Part 1. Physical and Mineralogical Properties* (ed. C.A. Black), pp. 210-221.
726 American Society of Agronomy, Madison.
727 Koerselman, W. (1989) Groundwater and surface water hydrology of a small groundwater-fed fen.
728 *Wetlands Ecology and Management*, **1**, 31-43.
729 Kruschke, J.K. (2011) *Doing Bayesian Data Analysis: A Tutorial with R and BUGS*. Elsevier,
730 Amsterdam.
731 Legendre, P. & Legendre, L. (1998) *Numerical Ecology*. Second edition, Elsevier, Amsterdam.

Lewis, C., Albertson, J.D., Xu, X. & Kiely, G. (2012) Spatial variability of hydraulic conductivity and bulk density along a blanket peatland hillslope. *Hydrological Processes*, **26**, 1527-1537.

Mauquoy, D., Hughes, P.D.M. & van Geel, B. (2010) A protocol for plant macrofossil analysis of peat deposits. *Mires and Peat*, **7**, 6.

Mauquoy, D., Yeloff, D., van Geel, B., Charman, D.J. & Blundell, A. (2008) Two decadally resolved records from north-west European peat bogs show rapid climate changes associated with solar variability during the mid–late Holocene. *Journal of Quaternary Science*, **23**, 745-763.

Minchin, P.R. (1987) An evaluation of the relative robustness of techniques for ecological ordination. *Vegetatio*, **69**, 89-107.

Morris, P.J., Baird, A.J. & Belyea, L.R. (2012) The DigiBog peatland development model 2: Ecohydrological simulations in 2D. *Ecohydrology*, **5**, 256-268.

Morris, P.J., Baird, A.J. & Belyea, L.R. (2013) The role of hydrological transience in peatland pattern formation. *Earth Surface Dynamics*, **1**, 29-43.

Morris, P.J., Baird, A.J. & Belyea, L.R. (2015) Bridging the gap between models and measurements of peat hydraulic conductivity. *Water Resources Research*, **51**, 5353-5364.

Morris, P.J., Waddington, J.M., Benscoter, B.W. & Turetsky, M.R. (2011) Conceptual frameworks in peatland ecohydrology: looking beyond the two-layered (acrotelm–catotelm) model. *Ecohydrology*, **4**, 1-11.

Oksanen, J., Blanchet, F.G., Kindt, R., Legendre, P., Minchin, P.R., O'Hara, R.B., Simpson, G.L., Solymos, P., Stevens, M.H.H. & Wagner, H. (2012) *vegan: Community Ecology Package*. R package version 2.0-5. URL: http://CRAN.R-project.org/package=vegan.

Quinton, W.L., Hayashi, M., & Carey, S.K. 2008. Peat hydraulic conductivity in cold regions and its relation to pore size and geometry. *Hydrological Processes*, **22**, 2829-2837.

R Core Team. (2012) *R: A Language and Environment for Statistical Computing*. R Foundation for Statistical Computing, Vienna, Austria. ISBN 3-900051-07-0, URL: http://www.R-project.org/.

Reimer, P.J., Baillie, M.G.L., Bard, E., Bayliss, A., Beck, J.W., Blackwell, P.G., Bronk Ramsey, C., Buck, C.E., Burr, G.S., Edwards, R.L., Friedrich, M., Grootes, P.M., Guilderson, T.P., Hajdas, I., Heaton, T.J., Hogg, A.G., Hughen, K.A., Kaiser, K.F., Kromer, B., McCormac, F.G., Manning, S.W., Reimer, R.W., Richards, D.A., Southon, J.R., Talamo, S., Turney, C.S.M., van der Plicht, J. & Weyhenmeyer, C.E. (2009) IntCal09 and Marine09 radiocarbon age calibration curves, 0-50,000 years Cal BP. *Radiocarbon*, **51**, 1111-1150.

Roulet, N.T., Lafleur, P.M., Richard, P.J.H., Moore, T.R., Humphreys, E.R. & Bubier, J. (2007) Contemporary carbon balance and late Holocene carbon accumulation in a northern peatland. *Global Change Biology*, **13**, 397-411, doi: 10.1111/j.1365-2486.2006.01292.x.

Rydin, H. & Jeglum, J. (2006) *The Biology of Peatlands*. Oxford University Press, Oxford.

Schulz, J. (2004) *Palaeoecological Approach using High-Resolution Macrofossil Analysis*, PhD thesis, University. of Southampton, Southampton, UK.

Surridge, B.W.J., Baird, A.J. & Heathwaite, A.L. (2005) Evaluating the quality of hydraulic conductivity estimates from piezometer slug tests in peat. *Hydrological Processes*, **19**, 1227-1244.

Suzuki, R. & Shimodaira, H. (2006). Pvclust: an R package for assessing the uncertainty in hierarchical clustering. *Bioinformatics*, **22**, 1540-1542.

Swanson, D.K. & Grigal, D.F. (1988) A simulation model of mire patterning. *Oikos*, **53**, 309-314.

Swindles, G.T., Morris, P.J., Baird, A.J., Blaauw, M. & Plunkett, G. (2012) Ecohydrological feedbacks confound peat-based climate reconstructions. *Geophysical Research Letters*, **39**, L11401.

780 Whittington, P.N. & Price, J.S. (2006) The effects of water table draw-down (as a surrogate for
781 climate change) on the hydrology of a fen peatland, Canada. *Hydrological Processes*, **20**,
782 3589-3600.
783 Winston, R.B. (1994) Models of the geomorphology, hydrology, and development of domed peat
784 bodies. *Geological Society of America Bulletin*, **106**, 1594-1604.

Table 1. Summary of the Bayesian pairwise comparisons of the *K* data

	R1 0.5	R2 0.5	H1 0.5	H2 0.5	R1 0.9	R2 0.9	H1 0.9	H2 0.9
R1 0.5		**1.07, 3.79**	**2.72, 6.67**	**3.11, 6.87**	**0.69,3.53**	**1.29, 4.09**	**3.06, 5.87**	**1.90, 4.58**
R2 0.5			**0.34, 4.19**	**0.73, 4.38**	-1.77, 1.07	-1.16, 1.6	**0.65, 3.36**	-0.48, 2.14
H1 0.5				-1.92, 2.46	**-4.60, -0.61**	**-3.99, -0.09**	-2.16, 1.64	-3.32, 0.44
H2 0.5					**-4.84, -1.07**	**-4.18, -0.48**	-2.32, 1.28	-3.52, 0.05
R1 0.9						-0.84, 2.06	**0.92, 3.8**	-0.21, 2.56
R2 0.9							**0.33, 3.13**	-0.75, 1.94
H1 0.9								-2.55, 0.08

Note. R1 and R2: Ridges 1 and 2; H1 and H2: Hollows 1 and 2. 0.5: 0.5 m depth. 0.9: 0.9 m depth. The numbers indicate the limits of the 95% highest density interval (HDI). If these do not include zero, there is a credible difference between the groups (which is also indicated in bold). See text for further details. Positive values suggest that a row has a lower *K* value than a column.

Table 2. Details of the ^{14}C dates obtained from Hollow 2 and Ridge 2

Lab. no.	Code	Depth (m)	Material	^{14}C age	+/-	AMS $\delta^{13}C$	Cal. 2σ range BP
UBA-20982	CFH2.30	0.2-0.3	*Sphagnum* leaves/branches/stems	82	21	-30.5	138- -4
UBA-20983	CFH2.60	0.5-0.6	*Sphagnum* leaves/branches/stems	477	24	-25.2	536-502
UBA-20984	CFH2.100	0.9-1.0	*Sphagnum* leaves/branches/stems	1206	21	-24.1	1179-1062
UBA-20985	CFR2.30	0.2-0.3	*Sphagnum* leaves/branches/stems	321	21	-25.9	460-307
UBA-20986	CFR2.60	0.5-0.6	*Sphagnum* leaves/branches/stems	1081	22	-26.1	1054-934
UBA-20987	CFR2.100	0.9-1.0	*Racomitrium* moss	1425	19	-23.1	1297-1315

Note. In the Code column CFH2 refers to Cors Fochno Hollow 2 and CFR2 refers to Cors Fochno Ridge 2.

802 **Figure captions**

803

804 **Figure 1**. Aerial photograph of the study area. The thick dashed line shows the location of the
805 transect used by Kettridge *et al*. (2012), with the northernmost part of the line representing the start
806 of the transect. The fine dashed lines delineate the areas from which the *K* readings were taken. The
807 hollows were larger than the areas shown, but measurements were restricted to those parts of the
808 hollows that contained the greatest cover of *Sphagnum pulchrum*.

809

810 **Figure 2.** Example of the apparently stalled response of some of the 0.5-m piezometers installed in
811 Ridge 1. The piezometer water levels shown here are atmospherically-corrected. The arrow shows
812 the assumed t_{95}. The grey dashed line indicates how background pore-water pressure may have
813 fallen during the test (due to water flow through the bog and evaporative losses).

814

815 **Figure 3.** The values of hydraulic conductivity (*K*) for each microform and depth. $n = 5$ in each
816 case, but over-plotting of similar values hides some symbols. All values are corrected to 20°C. Also
817 shown are the ranges of *K* values found (i) in the uppermost 0.3 m from the central patterned area of
818 the study site (unpublished data), and (ii) in the uppermost 0.5 m from a selection of raised and
819 blanket bogs (see the named studies). The *K* range given for the near-surface peat at the study site is
820 based on values corrected to 20°C; the minimum of this range is 4.8×10^{-8} m s^{-1}. *K* was measured at
821 a temperature of 18°C by Lewis *et al*. (2011), and their *K* values have been corrected to 20°C in the
822 figure. The *K* values from the other studies are not temperature-corrected.

823

824 **Figure 4.** Age-depth curves for Hollow 2 and Ridge 2. The curves show the maximum probability
825 ages from the Bayesian age-depth models.

826

827 **Figures 5a and b.** Macrofossil, humification, and dry bulk density data for three separate cores that
828 were taken from the centre of each microform. In the macrofossil part of each figure the ⦸ symbol
829 indicates a null return (the macrofossil concerned was absent throughout the core). The pale grey
830 bands indicate the depth intervals over which the *K* tests were done. Dry bulk densities are shown
831 by filled circles joined by a dotted line, von Post scores by a continuous line with no symbols.
832
833 **Figure 6.** Cluster dendrogram of the plant macrofossil data. The initial letter and first digit of the
834 sample codes refer to ridge (R) or hollow (H) and replicate (R1, R2, H1, H2). The remaining digit
835 or digits refer(s) to sample depth in m multiplied by 10 (so a depth in the figure of 1 is 0.1 m).
836
837 **Figure 7.** NMDS ordination biplots of plant macrofossil data (sample codes are the same as in Fig.
838 6). Species codes are abbreviated (see Figs 5a and 5b for the full names). NMDS axis 1 follows a
839 ridge-hollow/bog surface wetness gradient.
840

841 Figure 1.

842

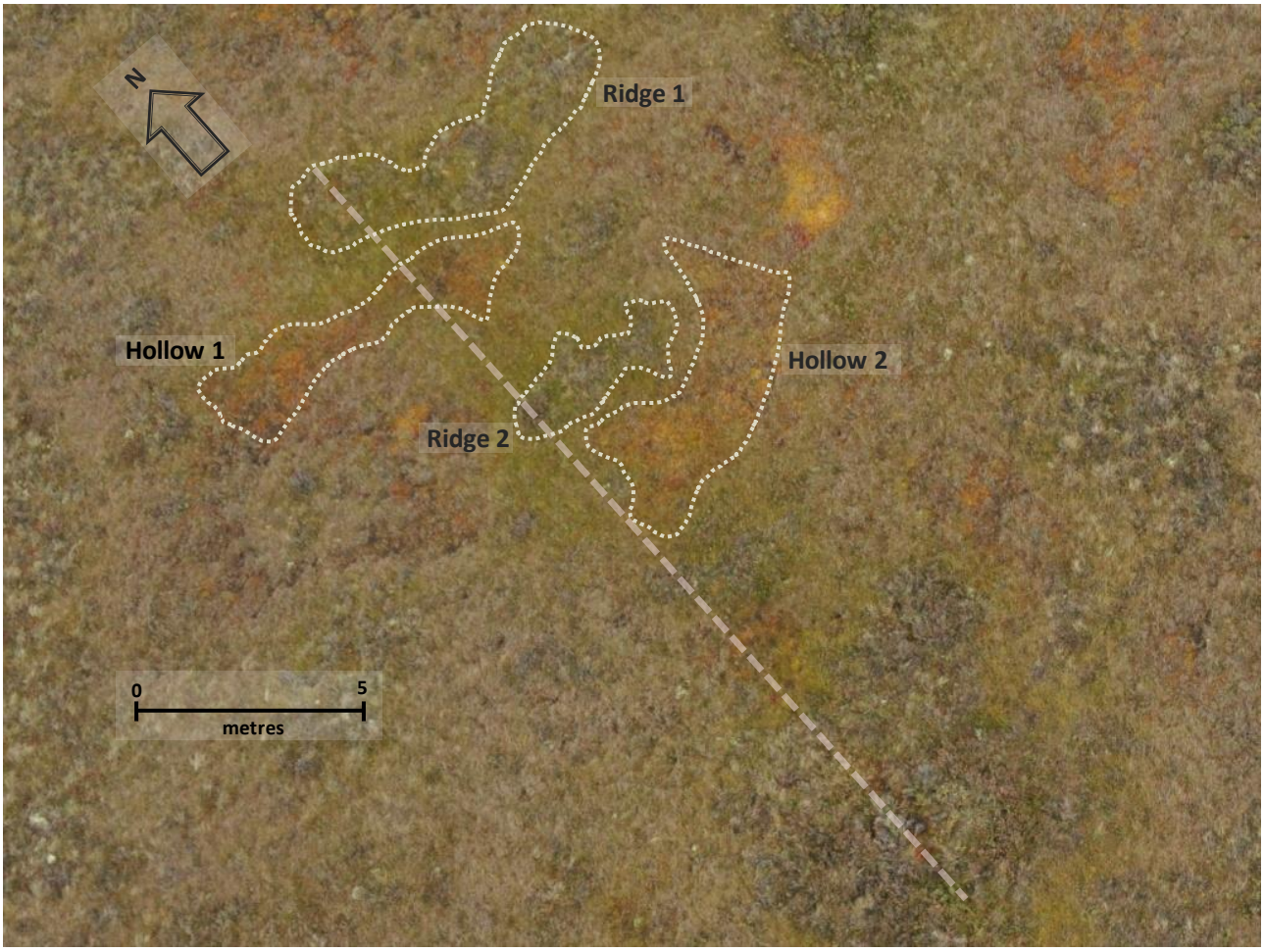

843

844

845

846 Figure 2.

847

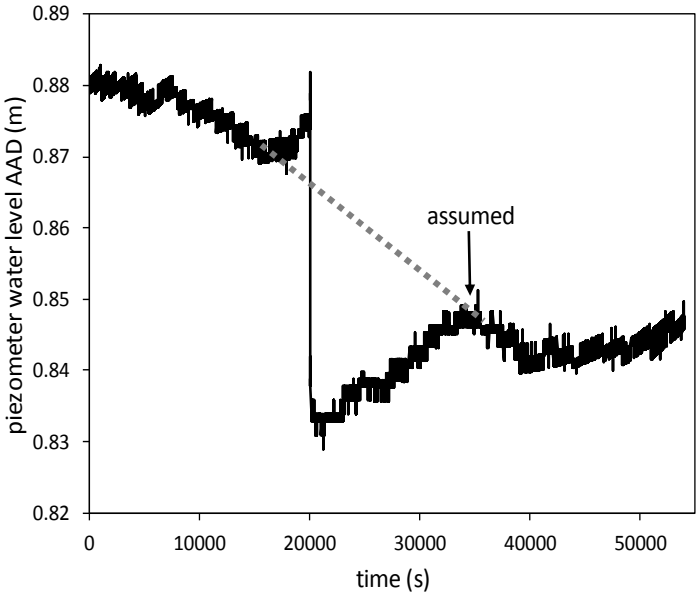

848

849

850

851

852 Figure 3.

853

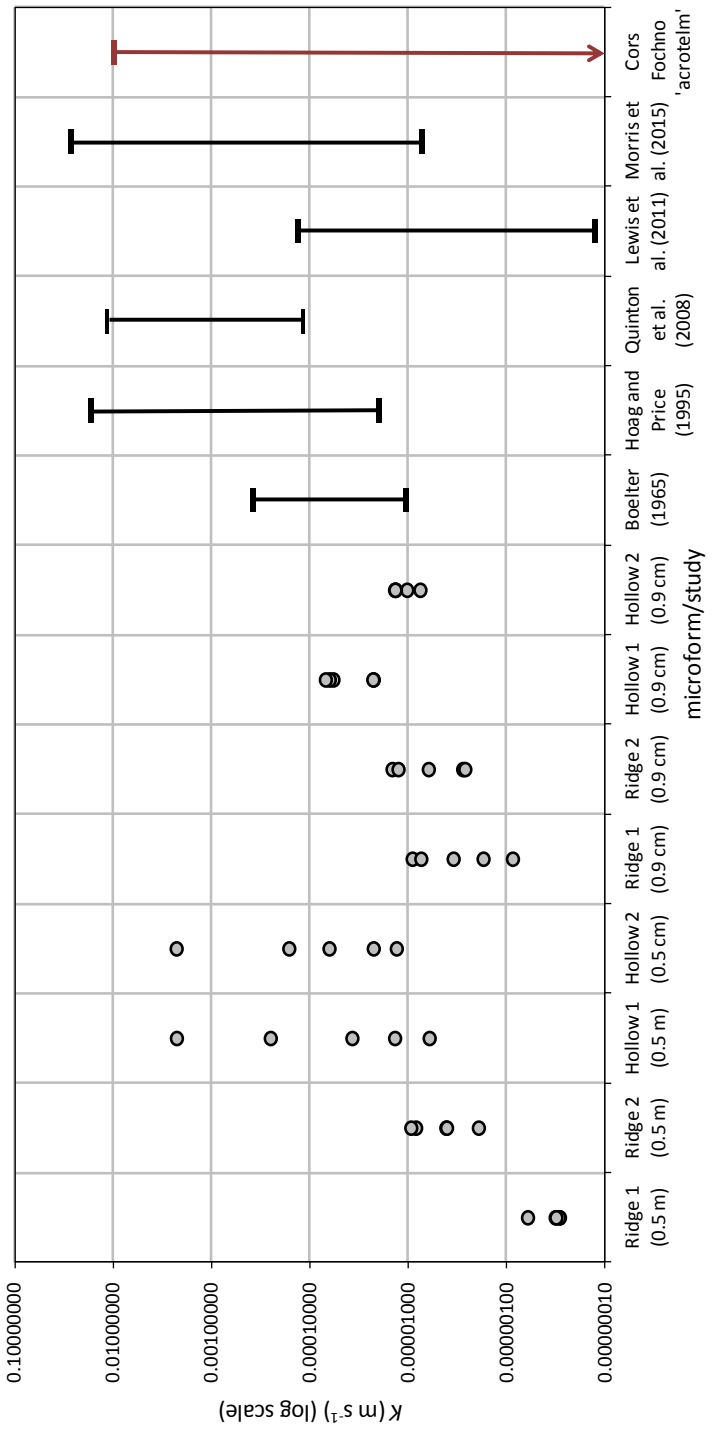

854

855

856 Figure 4.

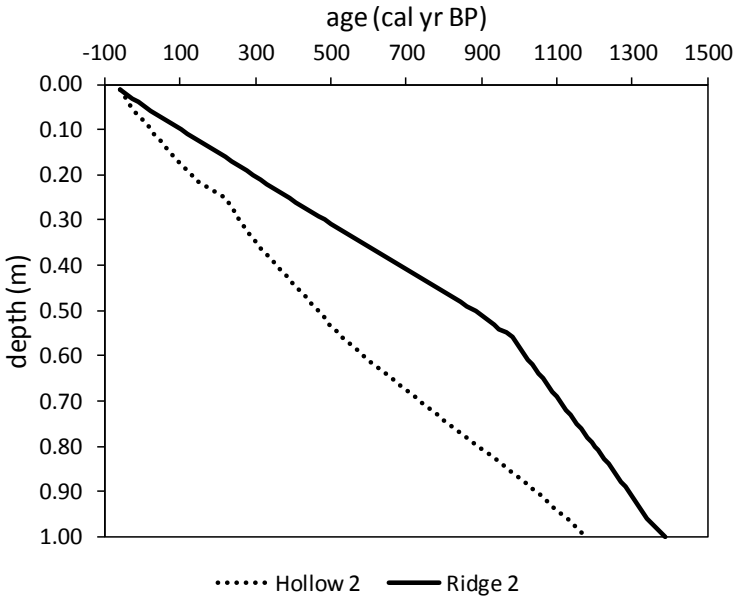

857

858

859

Figure 5a.

See separate pdf file.

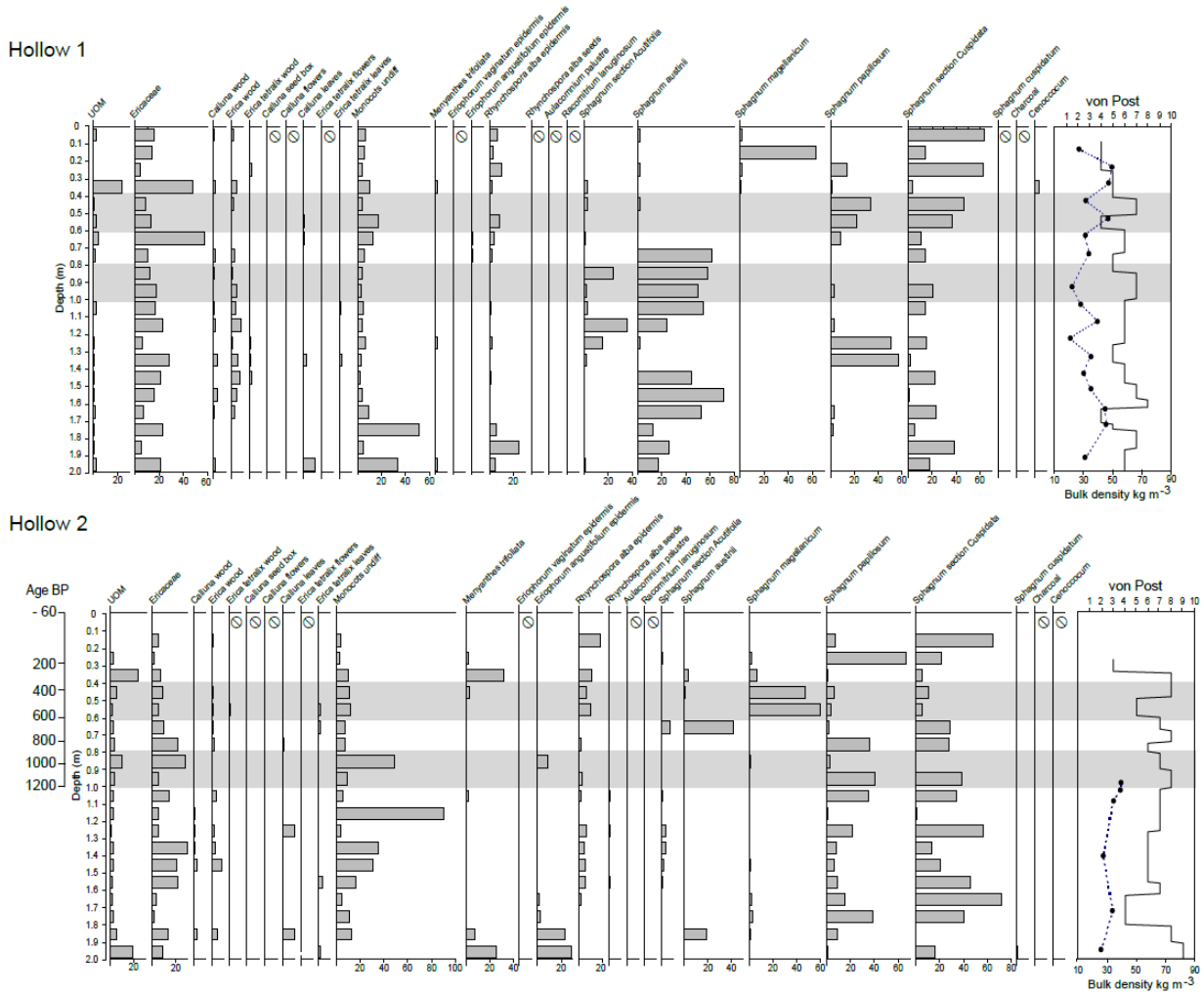

Figure 5b.

See separate pdf file.

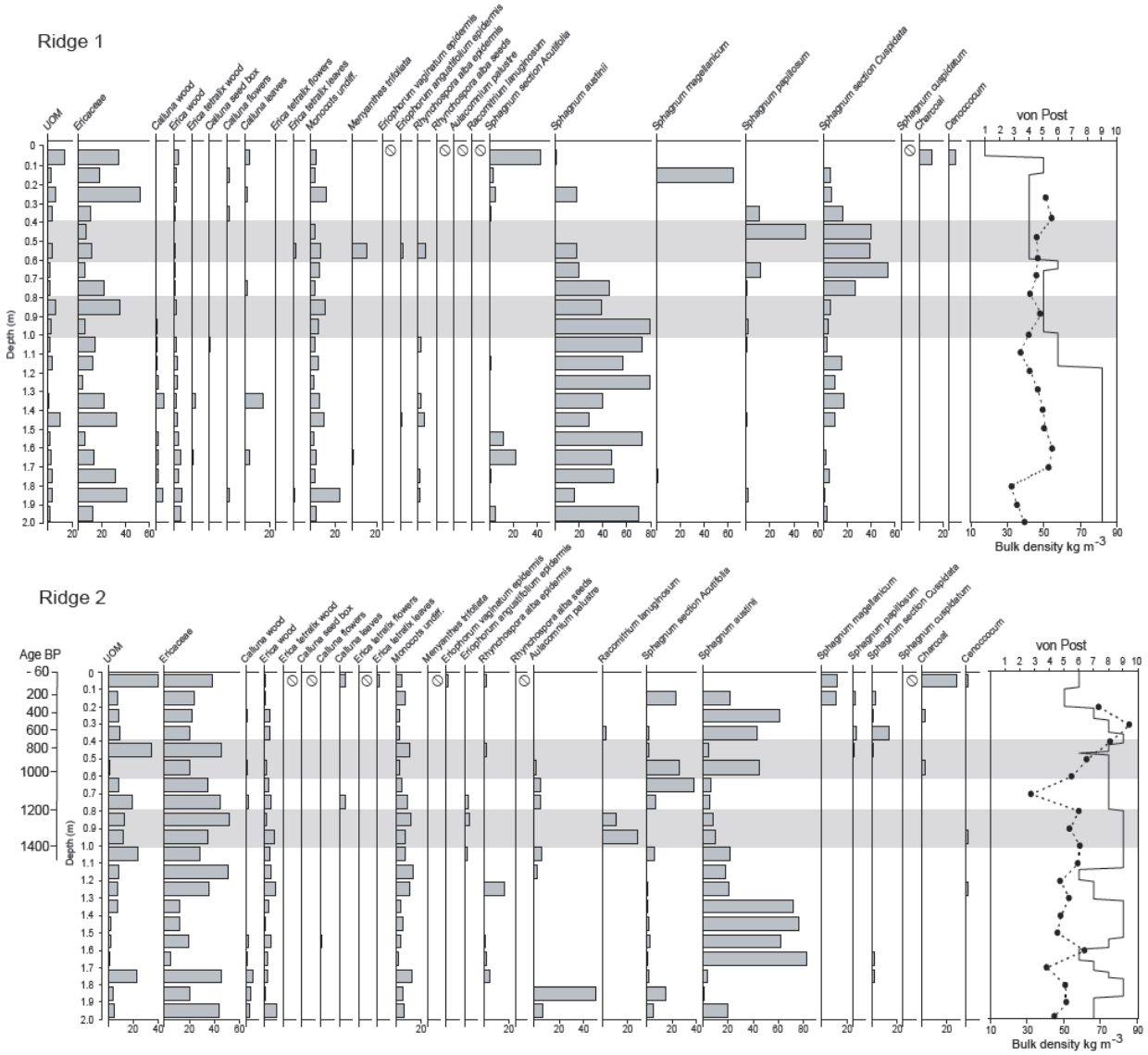

869 Figure 6.

870

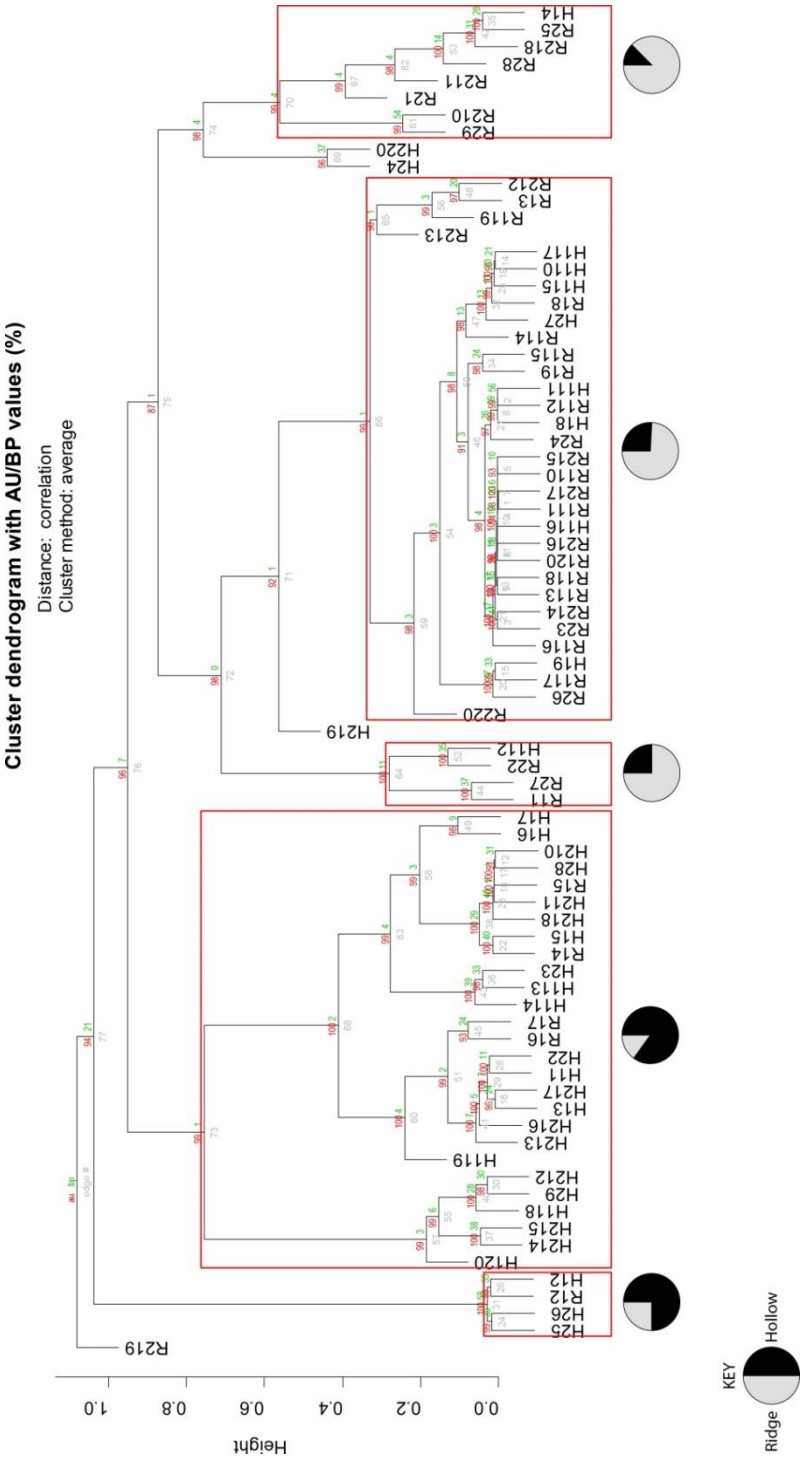

871

872

873

874 Figure 7.

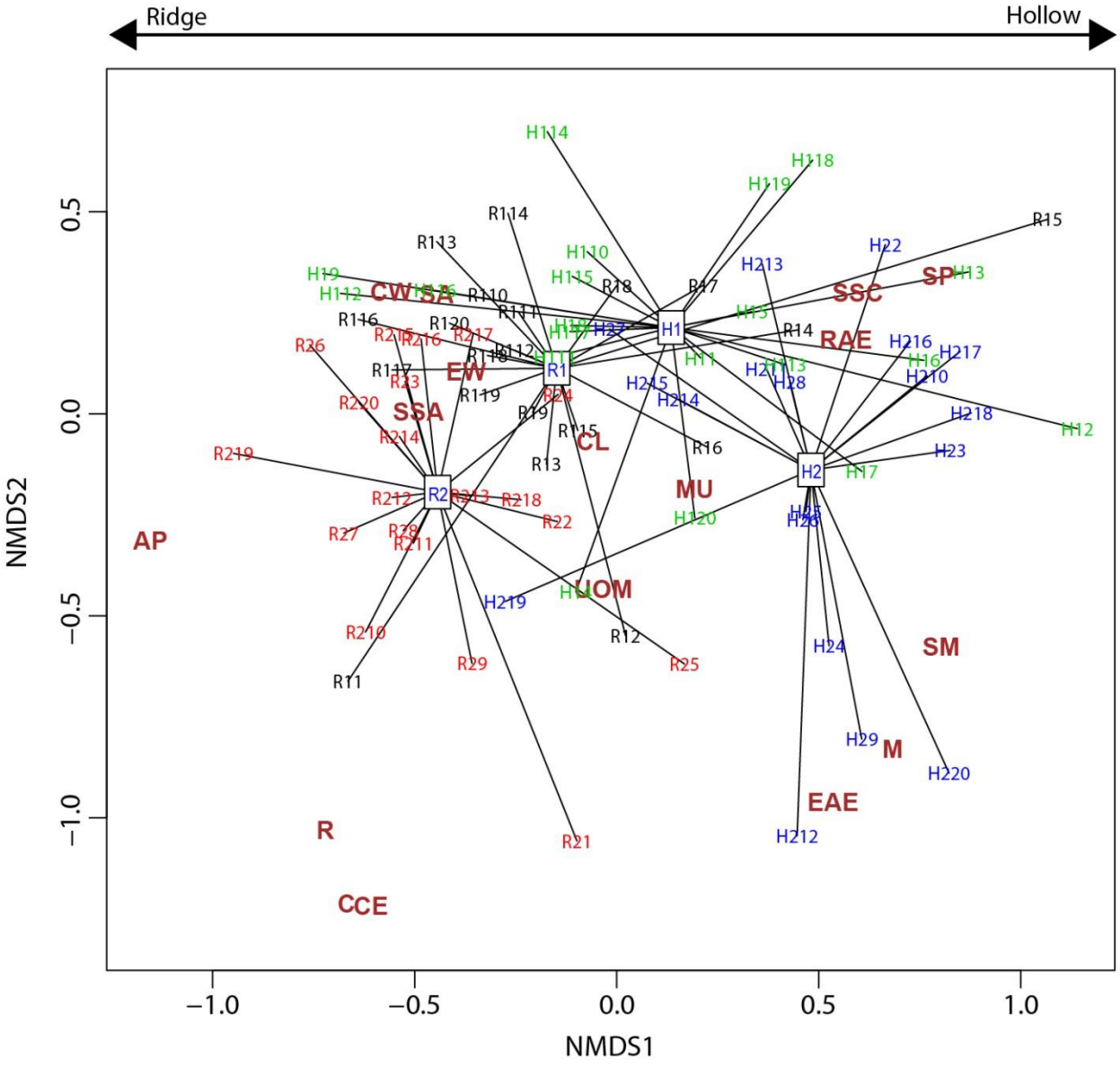

875

876

Microform-scale variations in peatland permeability and their ecohydrological implications

SUPPORTING INFORMATION

Web-based appendices S1-S5

Appendix S1: Botanical authorities and common names for the plant species named in the paper

Plant species	Botanical authority	Common name
Aulacomnium palustre	(Hedw.) Schwägr.	Bog Bead-moss
Calluna vulgaris	L.	Heather or Ling
Erica tetralix	L.	Cross-leaved Heath
Eriophorum angustifolium	Honck	Common Cottongrass
Eriophorum vaginatum	L.	Hare's Tail Cottongrass
Menyanthes trifoliata	L.	Bog Bean
Myrica gale	L.	Bog Myrtle
Racomitrium lanuginosum	Brid.	Woolly Fringe-moss
Rhododendron groenlandicum [formerly *Ledum groenlandicum*]	(Oeder) Kron & Judd [Oeder]	Labrador Tea
Rhynchospora alba	(L.) Vahl.	White-beaked Sedge
Sphagnum austinii	Sull.	Austin's Bog-moss
Sphagnum capillifolium	(Ehrh.) Hedw.	Acute-leaved Bog-moss
Sphagnum cuspidatum	Ehrh. ex Hoffm.	Feathery Bog-moss
Sphagnum fuscum	(Schimp.) Klinggr.	Rusty Bog-moss
Sphagnum magellanicum	Brid.	Magellanic Bog-moss
Sphagnum papillosum	Lindb.	Papillose Bog-moss
Sphagnum pulchrum	(Lindb. ex Braithw.) Warnst.	Golden Bog-moss

Appendix S2: The consistency of the piezometer tests

Three repeats were done on piezometers 23, 32, and 39, which were placed at a nominal depth of 0.5 m in Ridge 1, Ridge 2, and Hollow 2 respectively. Each repeat test was done within a day of the first test, and the results from both tests are shown in the three figures below. In piezometers 23 and 39 head recovery in the repeat test was similar to recovery to the first test, although for instrument 39 the second test took 60 % longer to reach $h/h_0 = 0.05$. In piezometer 32 the second test showed a much slower response than the first. It is unusual for repeat tests to be done on piezometers, especially over such short intervals, and it is difficult to put the results into a wider context. In piezometer tests on fen and bog peats, Rosa & Larocque (2008) report little between-test variability. They reproduce results from one piezometer installed in a fen peat that show very similar recoveries for the first and the repeat tests. Some tests done by Baird, Eades & Surridge (2008) in an earlier study of the permeability of the bog peat at Cors Fochno show variation between first and second tests that is similar to that found in the current study. However, most of the repeat tests carried out by Baird, Eades & Surridge (2008), from a total of 12 piezometers, tended to give similar responses to the first test, as with piezometer 23. Where Baird, Eades & Surridge (2008) found larger deviations, like that with piezometer 32 here, there was not a consistent pattern in terms of responses becoming progressively slower or faster. For example, in one of their piezometers, they found that the second test took more than twice as long as the first; however, a third test was much closer in duration to the first. It is difficult to explain the difference in response between second and first tests that occurs in some instruments, but it may be due to bubble migration and coalescence in the peat around the intake as discussed by Surridge, Baird & Heathwaite (2005). The same cautionary note as given by Baird, Eades & Surridge (2008) applies here: our results should be interpreted with an appreciation that substantial between-test variability is possible in individual instruments, although it seems that most instruments (piezometer 23 and the majority of the 12 piezometers that Baird, Eades & Surridge (2008) conducted repeat tests on) show little such variability.

Figures: Results from the replicate head-recovery tests conducted on piezometers 23 (upper: 0.5 m, Hollow 2), 32 (middle: 0.5 m, Ridge 2) and 39 (lower: 0.5 cm, Ridge 1) (lower). In each case the grey line is the first test.

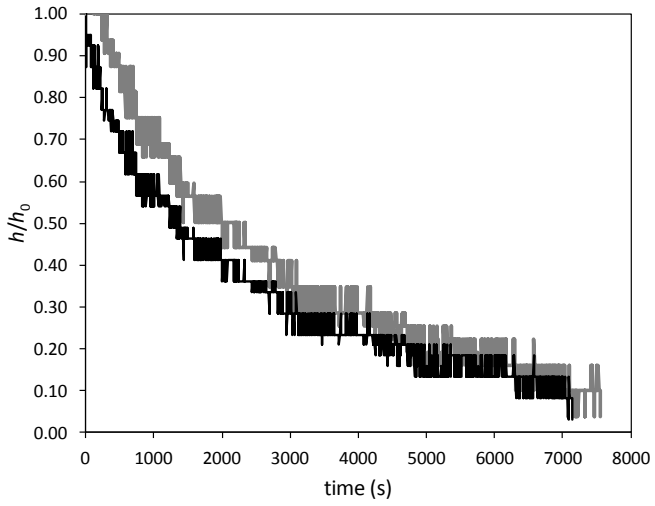

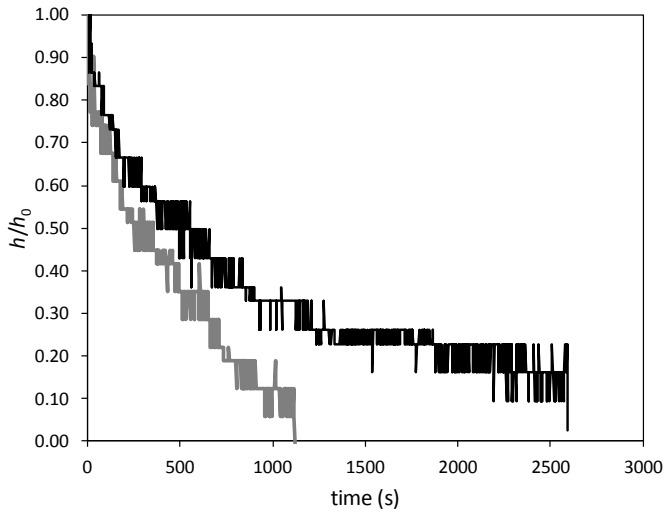

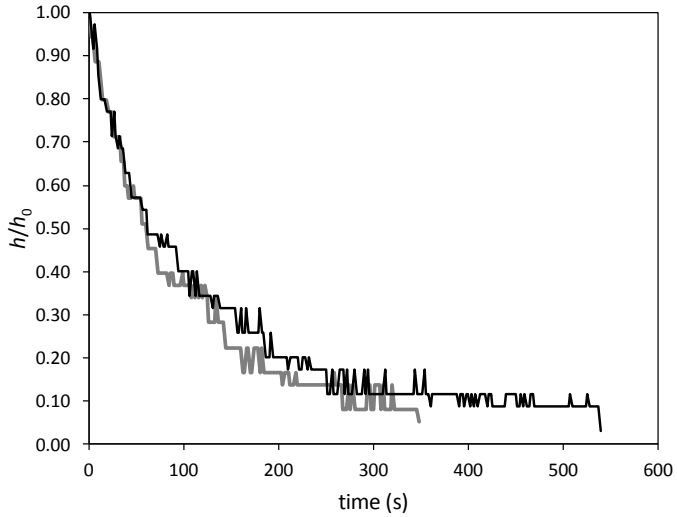

Baird, A.J., Eades, P.A. & Surridge, B.W.J. (2008) The hydraulic structure of a raised bog and its implications for ecohydrological modelling of bog development. *Ecohydrology*, **1**, 289-298.

Rosa, E. & Larocque, M. (2008) Investigating peat hydrological properties using field and laboratory methods: application to the Lanoraie peatland complex (southern Quebec, Canada). *Hydrological Processes*, **22**, 1866-1875.

Surridge, B.W.J., Baird, A.J. & Heathwaite, A.L. (2005) Evaluating the quality of hydraulic conductivity estimates from piezometer slug tests in peat. *Hydrological Processes*, **19**, 1227-1244.

Appendix S3: The Bayesian pair-wise comparison analysis

The JAGS (Just Another Gibbs Sampler) and R code used to undertake the Bayesian pairwise comparison of the permeability data is modified from the original (ANOVAonewayNonhomogvarJagsSTZ) available at:

http://www.indiana.edu/~kruschke/DoingBayesianDataAnalysis/Programs/ANOVAonewayNonhomogvarJagsSTZ.R

and at

https://github.com/pommedeterresautee/doingBayesianDataAnalysis/blob/master/ANOVAonewayNonhomogvarJagsSTZ.R

Both were last accessed on 2nd July 2015.

The code used is reproduced below.

```
rm(list=ls())  # Careful! This clears all of R's memory!
graphics.off() # This closes all of R's graphics windows.

graphics.off()
rm(list=ls(all=TRUE))

source("openGraphSaveGraph.R")
source("plotPost.R")
fileNameRoot="ANOVAonewayNonhomogvarJagsSTZ" # for constructing output filenames
require(rjags)          # Kruschke, J. K. (2011). Doing Bayesian Data Analysis:
                        # A Tutorial with R and BUGS. Academic Press / Elsevier.
#------------------------------------------------------------------------------
# THE MODEL.

modelstring = "
model {
  for ( i in 1:Ntotal ) {
    y[i] ~ dnorm( mu[i] , tau[x[i]] )
    mu[i] <- a0 + a[x[i]]
  }
  a0 ~ dnorm(0,0.001)
  for ( j in 1:NxLvl ) {
     a[j] ~ dnorm( 0.0 , atau )
     tau[j] ~ dgamma( sG , rG )
  }
  sG <- pow(m,2)/pow(d,2)
  rG <- m/pow(d,2)
  m ~ dgamma(1,1)
  d ~ dgamma(1,1)
```

```
    atau <- 1 / pow( aSD , 2 )
    aSD <- abs( aSDunabs ) + .1
    aSDunabs ~ dt( 0 , 0.001 , 2 )
    # Convert a0,a[] to sum-to-zero b0,b[] :
    for ( j in 1:NxLvl ) { mpred[j] <- a0 + a[j] }
    b0 <- mean( mpred[1:NxLvl] )
    for ( j in 1:NxLvl ) { b[j] <- mpred[j] - b0 }
  }
  " # close quote for modelstring
  # Write model to a file, and send to BUGS:
  writeLines(modelstring,con="model.txt")

  #------------------------------------------------------------------------------
  # THE DATA.

  # Specify data source:
  dataSource = c( "lncorsfochno" )[1]

  #meta-data
  #A = Ridge 1 (0.5 m)
  #B = Ridge 2 (0.5 m)
  #C = Hollow 1 (0.5 m)
  #D = Hollow 2 (0.5 cm)
  #E = Ridge 1 (0.9 cm)
  #F = Ridge 2 (0.9 cm)
  #G = Hollow 1 (0.9 cm)
  #H = Hollow 2 (0.9 cm)

  # Load the data:

  if ( dataSource == "lncorsfochno" ) {
    fileNameRoot = paste( fileNameRoot , dataSource , sep="" )
    datarecord = read.csv( "lncorsfochno.csv" )
    y = datarecord$Y
    Ntotal = length(y)
    x = as.numeric(datarecord$Group)
    xnames = levels(datarecord$Group)
    NxLvl = length(levels(datarecord$Group))
    normalize = function( v ){ return( v / sum(v) ) }
    contrastList = list(
      BvA = (xnames=="B")-(xnames=="A") ,
      CvA = (xnames=="C")-(xnames=="A") ,
      DvA = (xnames=="D")-(xnames=="A") ,
      EvA = (xnames=="E")-(xnames=="A") ,
      FvA = (xnames=="F")-(xnames=="A") ,
      GvA = (xnames=="G")-(xnames=="A") ,
      HvA = (xnames=="H")-(xnames=="A") ,
      CvB = (xnames=="C")-(xnames=="B") ,
      DvB = (xnames=="D")-(xnames=="B") ,
      EvB = (xnames=="E")-(xnames=="B") ,
      FvB = (xnames=="F")-(xnames=="B") ,
      GvB = (xnames=="G")-(xnames=="B") ,
      HvB = (xnames=="H")-(xnames=="B") ,
      DvC = (xnames=="D")-(xnames=="C") ,
      EvC = (xnames=="E")-(xnames=="C") ,
      FvC = (xnames=="F")-(xnames=="C") ,
      GvC = (xnames=="G")-(xnames=="C") ,
      HvC = (xnames=="H")-(xnames=="C") ,
      EvD = (xnames=="E")-(xnames=="D") ,
      FvD = (xnames=="F")-(xnames=="D") ,
      GvD = (xnames=="G")-(xnames=="D") ,
      HvD = (xnames=="H")-(xnames=="D") ,
      FvE = (xnames=="F")-(xnames=="E") ,
```

```
    GvE = (xnames=="G")-(xnames=="E") ,
    HvE = (xnames=="H")-(xnames=="E") ,
    GvF = (xnames=="G")-(xnames=="F") ,
    HvF = (xnames=="H")-(xnames=="F") ,
    HvG = (xnames=="H")-(xnames=="G")
    )
}
# Specify the data in a form that is compatible with BRugs model, as a list:
ySDorig = sd(y)
yMorig = mean(y)
z = ( y - yMorig ) / ySDorig
dataList = list(
  y = z ,
  x = x ,
  Ntotal = Ntotal ,
  NxLvl = NxLvl
)

#------------------------------------------------------------------------------
# INTIALIZE THE CHAINS.

theData = data.frame( y=dataList$y , x=factor(x,labels=xnames) )
a0 = mean( theData$y )
a = aggregate( theData$y , list( theData$x ) , mean )[,2] - a0
tau = 1/(aggregate( theData$y , list( theData$x ) , sd )[,2])^2
initsList = list( a0 = a0 , a = a , tau = tau , m = mean( tau ) ,
                  d = sd( tau ) , aSDunabs = sd(a) )

#------------------------------------------------------------------------------
# RUN THE CHAINS

parameters = c( "a0" ,  "a" , "b0" , "b" , "tau", "m", "d", "aSD" )
adaptSteps = 1000              # Number of steps to "tune" the samplers.
burnInSteps = 5000            # Number of steps to "burn-in" the samplers.
nChains = 3                   # Number of chains to run.
numSavedSteps=100000           # Total number of steps in chains to save.
thinSteps=1                   # Number of steps to "thin" (1=keep every step).
nPerChain = ceiling( ( numSavedSteps * thinSteps ) / nChains ) # Steps per
chain.
# Create, initialize, and adapt the model:
jagsModel = jags.model( "model.txt" , data=dataList , inits=initsList ,
                        n.chains=nChains , n.adapt=adaptSteps )
# Burn-in:
cat( "Burning in the MCMC chain...\n" )
update( jagsModel , n.iter=burnInSteps )
# The saved MCMC chain:
cat( "Sampling final MCMC chain...\n" )
codaSamples = coda.samples( jagsModel , variable.names=parameters ,
                            n.iter=nPerChain , thin=thinSteps )
# resulting codaSamples object has these indices:
#   codaSamples[[ chainIdx ]][ stepIdx , paramIdx ]

#------------------------------------------------------------------------------
# EXAMINE THE RESULTS

checkConvergence = FALSE
if ( checkConvergence ) {
  openGraph(width=7,height=7)
  autocorr.plot( codaSamples[[1]] , ask=FALSE )
  show( gelman.diag( codaSamples ) )
  effectiveChainLength = effectiveSize( codaSamples )
  show( effectiveChainLength )
}
```

```
227
228  # Convert coda-object codaSamples to matrix object for easier handling.
229  # But note that this concatenates the different chains into one long chain.
230  # Result is mcmcChain[ stepIdx , paramIdx ]
231  mcmcChain = as.matrix( codaSamples )
232  chainLength = NROW(mcmcChain)
233
234  # Extract parameters:
235  aSDSample = mcmcChain[,"aSD"]
236  tauSample = array( 0 , dim=c( dataList$NxLvl , chainLength ) )
237  for ( xidx in 1:dataList$NxLvl ) {
238     tauSample[xidx,] = mcmcChain[, paste("tau[",xidx,"]",sep="") ]
239  }
240  a0Sample = mcmcChain[, "a0" ]
241  aSample = array( 0 , dim=c( dataList$NxLvl , chainLength ) )
242  for ( xidx in 1:dataList$NxLvl ) {
243     aSample[xidx,] = mcmcChain[, paste("a[",xidx,"]",sep="") ]
244  }
245  b0Sample = mcmcChain[, "b0" ]
246  bSample = array( 0 , dim=c( dataList$NxLvl , chainLength ) )
247  for ( xidx in 1:dataList$NxLvl ) {
248     bSample[xidx,] = mcmcChain[, paste("b[",xidx,"]",sep="") ]
249  }
250
251  # Convert from standardized b values to original scale b values:
252  b0Sample = b0Sample * ySDorig + yMorig
253  bSample = bSample * ySDorig
254  sigmaSample = 1/sqrt(tauSample) * ySDorig
255
256  # Plot aSD
257  openGraph(width=7,height=7)
258  layout( matrix(1:2,nrow=2) )
259  par( mar=c(3,1,2.5,0) , mgp=c(2,0.7,0) )
260  plotPost( aSDSample , xlab="aSD" , main="a SD"  , showMode=T )
261  saveGraph(file=paste(fileNameRoot,"SD",sep=""),type="eps")
262
263  # Plot b values:
264  openGraph(width=dataList$NxLvl*2.75,height=2.5)
265  layout( matrix( 1:dataList$NxLvl , nrow=1 ) )
266  par( mar=c(3,1,2.5,0) , mgp=c(2,0.7,0) )
267  for ( xidx in 1:dataList$NxLvl ) {
268      plotPost( bSample[xidx,]  ,
269                xlab=bquote(beta*1[.(xidx)]) ,
270                main=paste("x:",xnames[xidx])  )
271  }
272  saveGraph(file=paste(fileNameRoot,"b",sep=""),type="eps")
273
274  # Plot tau values:
275  openGraph(width=dataList$NxLvl*2.75,height=2.5)
276  layout( matrix( 1:dataList$NxLvl , nrow=1 ) )
277  par( mar=c(3,1,2.5,0) , mgp=c(2,0.7,0) )
278  for ( xidx in 1:dataList$NxLvl ) {
279      plotPost( tauSample[xidx,]  ,
280                xlab=bquote(tau[.(xidx)]) ,
281                main=paste("x:",xnames[xidx]) , showMode=T )
282  }
283  saveGraph(file=paste(fileNameRoot,"tau",sep=""),type="eps")
284
285  # Display contrast analyses
286  nContrasts = length( contrastList )
287  if ( nContrasts > 0 ) {
288     nPlotPerRow = 5
289     nPlotRow = ceiling(nContrasts/nPlotPerRow)
```

```
    nPlotCol = ceiling(nContrasts/nPlotRow)
    openGraph(width=3.75*nPlotCol,height=2.5*nPlotRow)
    layout( matrix(1:(nPlotRow*nPlotCol),nrow=nPlotRow,ncol=nPlotCol,byrow=T) )
    par( mar=c(4,0.5,2.5,0.5) , mgp=c(2,0.7,0) )
    for ( cIdx in 1:nContrasts ) {
        contrast = matrix( contrastList[[cIdx]],nrow=1) # make it a row matrix
        incIdx = contrast!=0
        histInfo = plotPost( contrast %*% bSample , compVal=0  ,
                 xlab=paste( round(contrast[incIdx],2) , xnames[incIdx] ,
                             c(rep("+",sum(incIdx)-1),"") , collapse=" " ) ,
                 cex.lab = 1.0 ,
                 main=paste( "X Contrast:", names(contrastList)[cIdx] ) )
    }
    saveGraph(file=paste(fileNameRoot,"xContrasts",sep=""),type="eps")
}

# Display data with posterior predictive distributions
openGraph(width=1.5*NxLvl,height=5)
plot(0,0,
     xlim=c(0.2,NxLvl+0.1) , xlab="X" ,
     xaxt="n" ,
     ylim=c(min(y)-0.2*(max(y)-min(y)),max(y)+0.2*(max(y)-min(y))) , ylab="Y" ,
     main="Data with Posterior Predictive Distrib.")
axis( 1 , at=1:NxLvl , lab=xnames )
for ( j in 1:NxLvl ) {
  yVals = y[x==j]
  points( rep(j,length(yVals))+runif(length(yVals),-0.03,0.03) ,
          yVals , pch=20 , cex=1.5 , col="red" )
  chainSub = round(seq(1,chainLength,length=20))
  for ( chnIdx in chainSub ) {
    m = b0Sample[chnIdx] + bSample[j,chnIdx]
    s = sigmaSample[j,chnIdx]
    yl = m-1.96*s
    yh = m+1.96*s
    ycomb=seq(yl,yh,length=201)
    ynorm = dnorm(ycomb,mean=m,sd=s)
    ynorm = 0.75*ynorm/max(ynorm)
    lines( j-ynorm , ycomb , col="skyblue" ) # col=chnIdx )
  }
}
saveGraph(file=paste(fileNameRoot,"PostPred",sep=""),type="eps")
```

The principal results from the analysis are reproduced below. These show pair-wise comparisons of the β_j values (see explanation in main paper). Labels are as follows: A - Ridge 1 (0.5 m), B - Ridge 2 (0.5 m), C - Hollow 1 (0.5 m), D - Hollow 2 (0.5 cm), E - Ridge 1 (0.9 cm), F - Ridge 2 (0.9 cm), G - Hollow 1 (0.9 cm), H - Hollow 2 (0.9 cm).

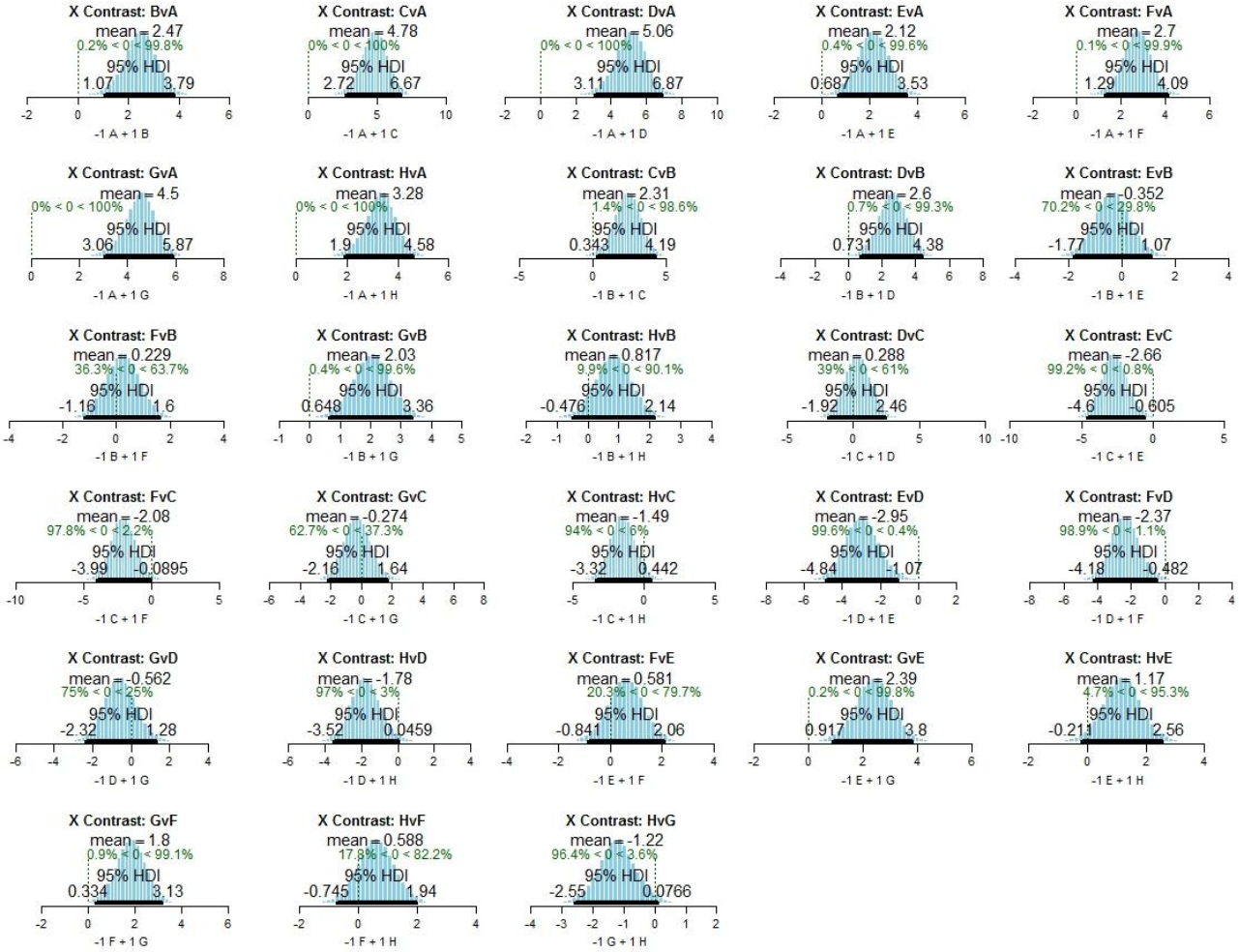
X Contrast: BvA
mean = 2.47
0.2% < 0 < 99.8%
95% HDI
1.07 3.79
-1 A + 1 B
X Contrast: CvA
mean = 4.78
0% < 0 < 100%
95% HDI
2.72 6.67
-1 A + 1 C
X Contrast: DvA
mean = 5.06
0% < 0 < 100%
95% HDI
3.11 6.87
-1 A + 1 D
X Contrast: EvA
mean = 2.12
0.4% < 0 < 99.6%
95% HDI
0.687 3.53
-1 A + 1 E
X Contrast: FvA
mean = 2.7
0.1% < 0 < 99.9%
95% HDI
1.29 4.09
-1 A + 1 F
X Contrast: GvA
mean = 4.5
0% < 0 < 100%
95% HDI
3.06 5.87
-1 A + 1 G
X Contrast: HvA
mean = 3.28
0% < 0 < 100%
95% HDI
1.9 4.58
-1 A + 1 H
X Contrast: CvB
mean = 2.31
1.4% < 0 < 98.6%
95% HDI
0.343 4.19
-1 B + 1 C
X Contrast: DvB
mean = 2.6
0.7% < 0 < 99.3%
95% HDI
0.731 4.38
-1 B + 1 D
X Contrast: EvB
mean = -0.352
70.2% < 0 < 29.8%
95% HDI
-1.77 1.07
-1 B + 1 E
X Contrast: FvB
mean = 0.229
36.3% < 0 < 63.7%
95% HDI
-1.16 1.6
-1 B + 1 F
X Contrast: GvB
mean = 2.03
0.4% < 0 < 99.6%
95% HDI
0.648 3.36
-1 B + 1 G
X Contrast: HvB
mean = 0.817
9.9% < 0 < 90.1%
95% HDI
-0.476 2.14
-1 B + 1 H
X Contrast: DvC
mean = 0.288
39% < 0 < 61%
95% HDI
-1.92 2.46
-1 C + 1 D
X Contrast: EvC
mean = -2.66
99.2% < 0 < 0.8%
95% HDI
-4.6 -0.605
-1 C + 1 E
X Contrast: FvC
mean = -2.08
97.8% < 0 < 2.2%
95% HDI
-3.99 -0.0895
-1 C + 1 F
X Contrast: GvC
mean = -0.274
62.7% < 0 < 37.3%
95% HDI
-2.16 1.64
-1 C + 1 G
X Contrast: HvC
mean = -1.49
94% < 0 < 6%
95% HDI
-3.32 0.442
-1 C + 1 H
X Contrast: EvD
mean = -2.95
99.6% < 0 < 0.4%
95% HDI
-4.84 -1.07
-1 D + 1 E
X Contrast: FvD
mean = -2.37
98.9% < 0 < 1.1%
95% HDI
-4.18 -0.482
-1 D + 1 F
X Contrast: GvD
mean = -0.562
75% < 0 < 25%
95% HDI
-2.32 1.28
-1 D + 1 G
X Contrast: HvD
mean = -1.78
97% < 0 < 3%
95% HDI
-3.52 0.0459
-1 D + 1 H
X Contrast: FvE
mean = 0.581
20.3% < 0 < 79.7%
95% HDI
-0.841 2.06
-1 E + 1 F
X Contrast: GvE
mean = 2.39
0.2% < 0 < 99.8%
95% HDI
0.917 3.8
-1 E + 1 G
X Contrast: HvE
mean = 1.17
4.7% < 0 < 95.3%
95% HDI
-0.211 2.56
-1 E + 1 H
X Contrast: GvF
mean = 1.8
0.9% < 0 < 99.1%
95% HDI
0.334 3.13
-1 F + 1 G
X Contrast: HvF
mean = 0.588
17.8% < 0 < 82.2%
95% HDI
-0.745 1.94
-1 F + 1 H
X Contrast: HvG
mean = -1.22
96.4% < 0 < 3.6%
95% HDI
-2.55 0.0766
-1 G + 1 H

338
339

340

Appendix S4: The Bayesian age-depth models for Hollow 2 and Ridge 2

The R code used to derive the age-depth models is as follows.

```
setdir("C:\Bacon").
source('Bacon.R')
Bacon("CF", acc.shape=2, acc.mean=13) # load CF data, define accumulation shape
and accumulation mean priors
ds <- seq(15, 20, length=10) # define the ages that describe the interval of
interest at a 'reasonable' resolution
ages <- c() # define a variable to contain the ages of said interval of depths
for(i in ds)# determine them from model
ages <- c(ages, Bacon.Age.d(i)) # assign them
hist(ages) # plot histogram of resulting ages of this depth interval
```

The graphs showing the analysis and the resulting models are given below. On the top panels of both graphs, leftmost plots show that both MCMC runs were stable (> 2000 iterations), middle plots show the prior (curves) and posterior (filled histograms) distributions for the accumulation rate (yr cm^{-1}), and the rightmost plots show the prior (curves) and posterior (filled histograms) for the dependence of accumulation rate between sections. The large plots show age distributions of calibrated ^{14}C dates and the age-depth model (grey-scale). Dark grey areas indicate precisely dated sections of the chronology, while lighter grey areas indicate less chronologically secure sections.

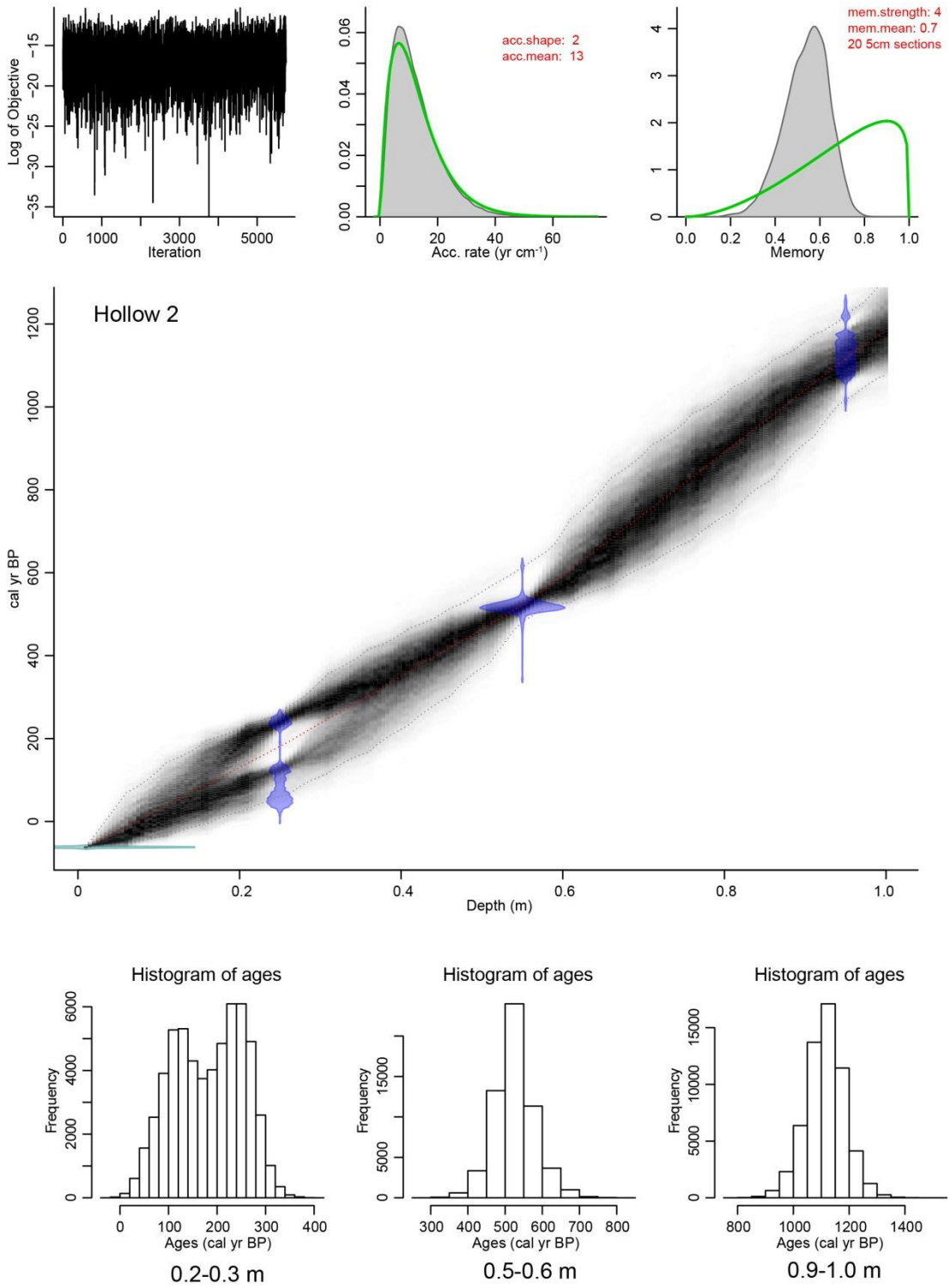
Log of Objective
Iteration
acc.shape: 2
acc.mean: 13
Acc. rate (yr cm-1)
mem.strength: 4
mem.mean: 0.7
20 5cm sections
Memory
Hollow 2
cal yr BP
Depth (m)
Histogram of ages
Frequency
Ages (cal yr BP)
0.2-0.3 m
0.5-0.6 m
0.9-1.0 m

363

364

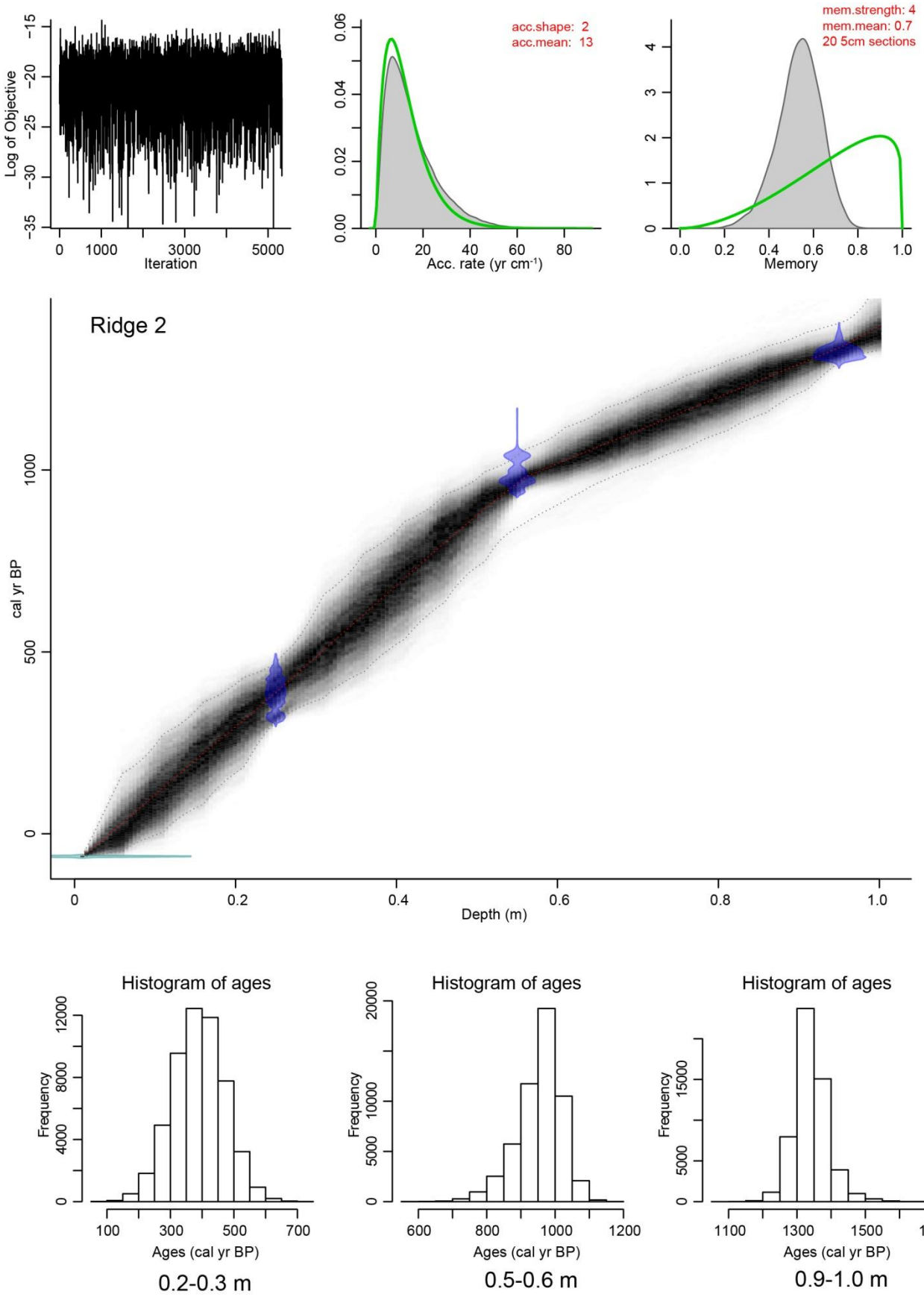
Log of Objective
Iteration
acc.shape: 2
acc.mean: 13
Acc. rate (yr cm-1)
mem.strength: 4
mem.mean: 0.7
20 5cm sections
Memory
Ridge 2
cal yr BP
Depth (m)
Histogram of ages
Frequency
Ages (cal yr BP)
0.2-0.3 m
Histogram of ages
Frequency
Ages (cal yr BP)
0.5-0.6 m
Histogram of ages
Frequency
Ages (cal yr BP)
0.9-1.0 m

365

366

Appendix S5: The von Post humification data from all three humification cores in each microform (the data from the central cores are also shown in Figs 5a and 5b in the main paper).

The western, central and eastern cores for each microform are shown from left to right.